Green’s function integral equation methods for plasmonic nanostructures

(PhD course: Optical at the nanoscale)

Thomas Søndergaard

Department of Physics and Nanotechnology
Aalborg University, Denmark

Outline

- Surface plasmon polaritons and plasmonic nanostructures
  - bandgap structures, gratings and resonators
- Green's tensor volume integral equation method (VIEM):
- Green's tensor area integral equation method (AIEM):
- Green's function surface integral equation method (SIEM):
- Summary

Introduction to surface plasmon polaritons

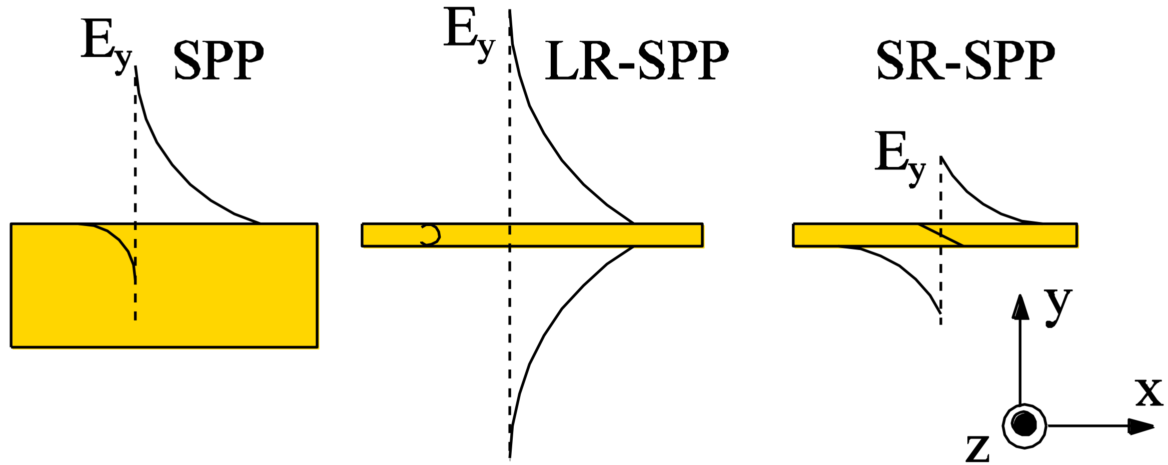

Examples of plasmonic nano structures

SPP bandgap structure LR-SPP grating SR-SPP resonator

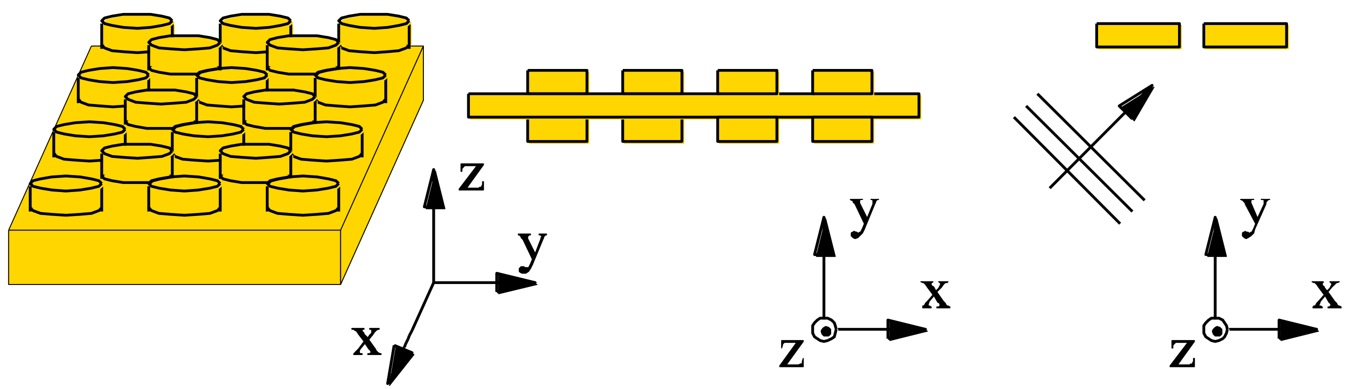

Green's tensor volume integral equation method (VIEM):

Vector wave equation: $\left(-\nabla\nabla\cdot+\nabla^2+k_0^2\varepsilon(\mathbf{r})\right)\mathbf{E}(\mathbf{r})=\mathbf{0}$

Boundary condition: $\mathbf{E}(\mathbf{r})=\mathbf{E}_0(\mathbf{r})+\mathbf{E}_{scat}(\mathbf{r})$

The given $\mathbf{E}_0$ satisfies: $\left(-\nabla\nabla\cdot+\nabla^2+k_0^2\varepsilon_{ref}(\mathbf{r})\right)\mathbf{E}_0(\mathbf{r})=\mathbf{0}$

Green's tensor $\mathbf{G}$: $\left(-\nabla\nabla\cdot+\nabla^2+k_0^2\varepsilon_{ref}(\mathbf{r})\right)\mathbf{G}(\mathbf{r},\mathbf{r}')=-\mathbf{I}\delta(\mathbf{r}-\mathbf{r}')$

By rewriting the vector wave equations for the incident and total field we find

$$\left(-\nabla\nabla\cdot+\nabla^2+k_0^2\varepsilon_{ref}(\mathbf{r})\right)\left(\mathbf{E}(\mathbf{r})-\mathbf{E}_0(\mathbf{r})\right)=-k_0^2\left(\varepsilon(\mathbf{r})-\varepsilon_{ref}(\mathbf{r})\right)\mathbf{E}(\mathbf{r})$$

which is satisfied by

$$\mathbf{E}(\mathbf{r})=\mathbf{E}_0(\mathbf{r})+\int\mathbf{G}(\mathbf{r},\mathbf{r}')\mathrm{k}_0^2\left(\varepsilon(\mathbf{r}')-\varepsilon_{\mathrm{ref}}(\mathbf{r}')\right)\cdot\mathbf{E}(\mathbf{r}')\mathrm{d}^3\mathrm{r}'$$

The solution where the scattered field $\mathbf{E}_{\mathrm{scat}}=(\mathbf{E}-\mathbf{E}_0)$ satisfies the radiating boundary condition is obtained if we choose the **G** which satisfies this condition

Green's tensor in the case of a homogeneous dielectric

$$\varepsilon_{ref}(\mathbf{r}) = \varepsilon_{ref} = n^2$$

$$\mathbf{G}(\mathbf{r},\mathbf{r}') = \mathbf{G}^{\mathrm{D}}(\mathbf{r}-\mathbf{r}') = \left(\frac{1}{k^2}\nabla\nabla + \mathbf{I}\right) g^{\mathrm{D}}(\mathbf{r}-\mathbf{r}')$$

$$k = k_0 n = \frac{2\pi}{\lambda_0} n$$

$$g^{\mathrm{D}}(\mathbf{r}-\mathbf{r}') = \frac{e^{-ik|\mathbf{r}-\mathbf{r}'|}}{4\pi|\mathbf{r}-\mathbf{r}'|} \quad , \quad \left(\nabla^2 + k^2\right) g^{\mathrm{D}}(\mathbf{r}-\mathbf{r}') = -\delta(\mathbf{r}-\mathbf{r}')$$

Green's tensor in the case of a planar metal-dielectric interface

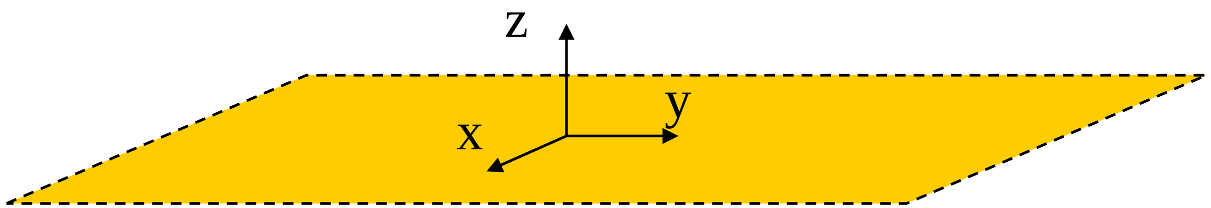

$$\mathbf{G}(\mathbf{r},\mathbf{r}') = \mathbf{G}^{\mathrm{D}}(\mathbf{r},\mathbf{r}') + \mathbf{G}^{\mathrm{S}}(\mathbf{r},\mathbf{r}')$$

$\mathbf{G}^{\mathrm{S}}$ can be calculated via Sommerfeld-integrals – example for z,z'>0

$$\hat{z}\cdot\mathbf{G}^{\mathrm{S}}\cdot\hat{z} = \frac{-i}{4\pi k_0^2 n_d^2}\int_0^\infty d\kappa_\rho \frac{\kappa_\rho^3}{\kappa_z} r^{(p)} J_0\left(\kappa_\rho \rho\right) e^{-i\kappa_z (z+z')},$$

$$\kappa_z = \sqrt{k_0^2 n_d^2 - \kappa_\rho^2}, \quad \rho = \left|\hat{x}\left(x-x'\right) + \hat{y}\left(y-y'\right)\right|, \quad \mathrm{Im}\left(\kappa_z\right) \leq 0$$

$r^{(p)} = r^{(p)}(\kappa_\rho)$: Fresnel reflection coefficient for p-polarized waves

Discretization of the Green's tensor volume integral equation

$$\mathbf{E}(\mathbf{r}) = \mathbf{E}_0(\mathbf{r}) + \int \mathbf{G}(\mathbf{r},\mathbf{r}')\mathrm{k}_0^2\left(\varepsilon(\mathbf{r}') - \varepsilon_{\mathrm{ref}}(\mathbf{r}')\right)\cdot \mathbf{E}(\mathbf{r}')\mathrm{d}^3\mathrm{r}'$$

Discretization approximation: constant field and material parameter assumed in each volume element

$$\mathbf{E}_i \approx \mathbf{E}_{0,i} + \sum_j \mathbf{G}_{ij}\cdot\left(\varepsilon_j - \varepsilon_{\mathrm{ref}}\right)\mathbf{E}_j \qquad \mathbf{G}_{ij} = \int_{V_j} \mathbf{G}(\mathbf{r}_i,\mathbf{r}')\mathrm{k}_0^2\mathrm{d}^3\mathrm{r}'$$

Case $i=j$: the singularity of **G** can be dealt with by transforming the integral into a surface integral away from the singularity

Discrete Dipole Approximation (DDA): $\mathbf{G}_{\mathrm{ij}} \approx \mathbf{G}(\mathbf{r}_{\mathrm{i}},\mathbf{r}_{\mathrm{j}})\mathrm{k}_0^2 V, \quad i \neq j$

Purcell and Pennypacker, 1973, used the equivalent of: $\mathbf{G}_{\mathrm{ii}} \approx -\dfrac{1}{3\varepsilon_{ref}}\mathbf{I}$

B.T. Draine, 1988, used the equivalent of: $\mathbf{G}_{\mathrm{ii}} \approx -\left(\dfrac{1}{3\varepsilon_{ref}} + i\dfrac{k^3 V}{6\pi\varepsilon_{ref}}\right)\mathbf{I}$

Green's tensor volume integral equation method (VIEM): self-interaction term / radiation reaction

For $i=j$ it is advantageous for the evaluation of G_{ii} to rewrite (part of the) volume integral as a surface integral

$$\int_{V_i} \mathbf{G}^{\mathrm{D}}(\mathbf{r}_{\mathrm{i}},\mathbf{r}')k^2 \mathrm{d}^3 r' = \int_{V_i} \left(\frac{1}{k^2}\nabla\nabla + \mathbf{I} \right) g^{\mathrm{D}}(\mathbf{r}_{\mathrm{i}},\mathbf{r}')k^2 \mathrm{d}^3 r'$$

$$= \int_{V_i} \left[\left(\nabla'\nabla' - \mathbf{I}\nabla'\cdot\nabla' \right) g^{\mathrm{D}}(\mathbf{r}_{\mathrm{i}},\mathbf{r}') - \delta(\mathbf{r}_{\mathrm{i}} - \mathbf{r}') \right] \mathrm{d}^3 r'$$

$$= -\mathbf{I} + \oint_{\partial V_i} \left(\hat{n}'\nabla' - \mathbf{I}\hat{n}'\cdot\nabla' \right) g^{\mathrm{D}}(\mathbf{r}_{\mathrm{i}},\mathbf{s}') \mathrm{d}^2 s'$$

Where we have used

$$\left(\nabla^2 + k^2 \right) g^{\mathrm{D}}(\mathbf{r},\mathbf{r}') = -\delta(\mathbf{r} - \mathbf{r}')$$

Taking advantage of the Fast Fourier Transform (FFT)

In e.g. the case where we use the DDA, or volume elements of the same *size* and *shape* placed on a cubic lattice, and a homogeneous background, the discretized equation to be solved takes the form of a discrete convolution

$$\mathbf{E}_{i_x,i_y,i_z} \approx \mathbf{E}_{0,i_x,i_y,i_z} + \sum_{j_x,j_y,j_z} \mathbf{G}^{\mathrm{D}}_{i_x-j_x,i_y-j_y,i_z-j_z} \cdot \left(\varepsilon_{j_x,j_y,j_z} - \varepsilon_{\mathrm{ref}}\right)\mathbf{E}_{j_x,j_y,j_z}$$

Gaussian elimination, LU-decomposition etc. scales as N^3
=> Matrix inversion is not efficient for large numbers of volume elements.

The equation is solved by an iterative approach where a trial vector containing $\mathbf{E}_{i_x,i_y,i_z}$ is optimized until a convergence criteria is satisfied. This procedure involves many matrix multiplications of the above form.

The convolution is carried out by the FFT, multiplication in reciprocal space, and another FFT. This procedure scales as $N\log N$.

Green's tensor volume integral equation method (VIEM):
- Modeling of a single surface scatterer

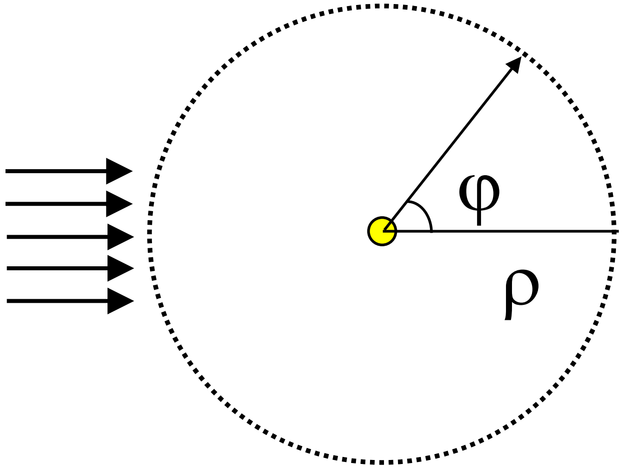

The magnitude of the scattered field is calculated at a small height above the surface but at a large distance ρ=10μm as a function of direction φ

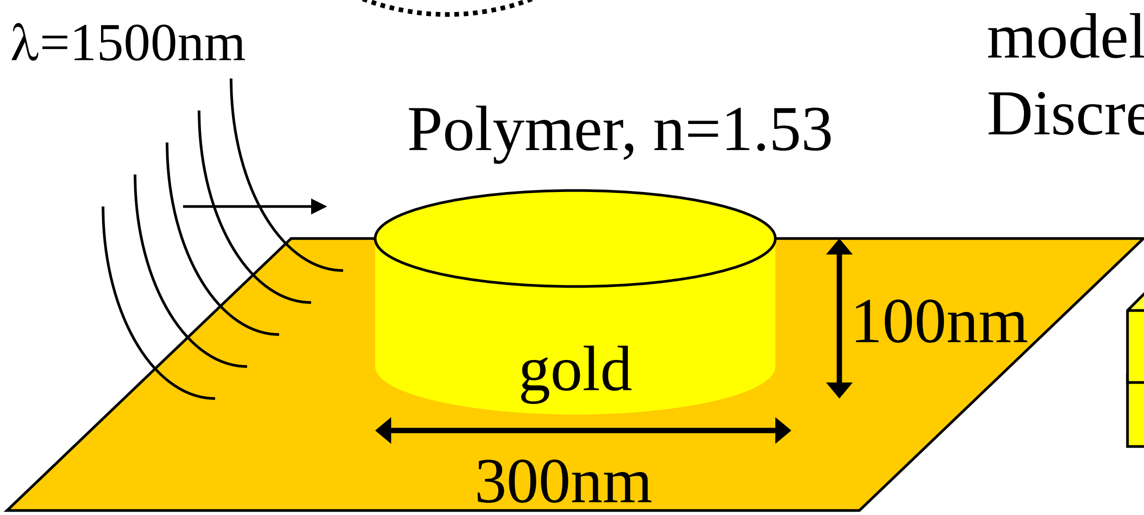

Actual structure being modeled when using cubic Discretization elements

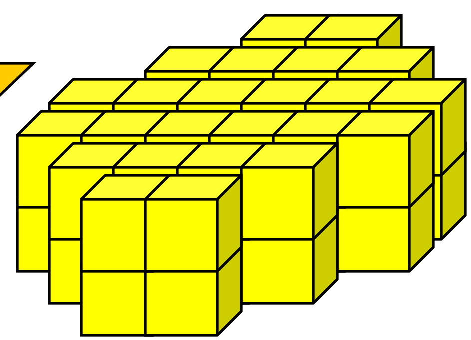

Poor convergence when using cubic discretization elements ☹

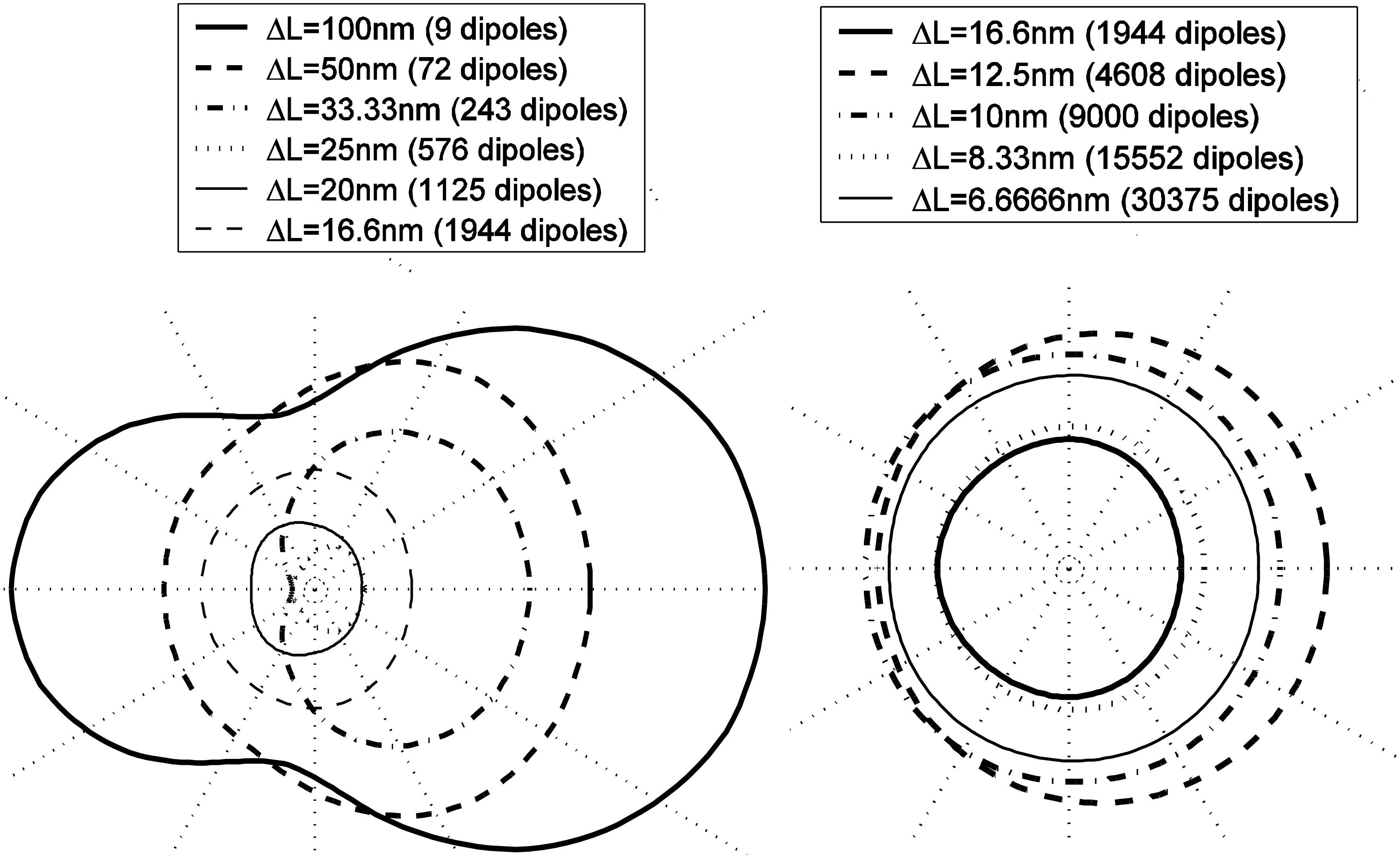

Green's tensor volume integral equation method (VIEM):

- Taking advantage of cylindrical symmetry by using a formulation of the VIEM based on ring discretization elements

The incident and total fields are expanded in angular momentum components:

$$\mathbf{E} = \sum_m \mathbf{E}^m(\mathbf{r}) \quad , \quad \mathbf{E}^m(\mathbf{r}) = \left(\hat{z} E_z^m(\rho, z) + \hat{\rho} E_\rho^m(\rho, z) + \hat{\phi} E_\phi^m(\rho, z) \right) e^{im\phi}$$

$$E_{p,i}^m = E_{p,i}^{0,m} + \sum_j \sum_{q,s=\rho,\phi,z} G_{pq,ij}^m k_0^2 \left(\varepsilon_{qs} - \delta_{qs} \right) E_{s,j}^m$$

$$p, q = \rho, \phi, z$$

$$\hat{p}, \hat{q} = \hat{\rho}, \hat{\phi}, \hat{z}$$

$$G_{pq,ij}^m = \int_{\text{ring } j} \hat{p} \cdot \mathbf{G}(\mathbf{r}_i, \mathbf{r}') \cdot \hat{q}' e^{im(\phi' - \phi_i)} d^3 r'$$

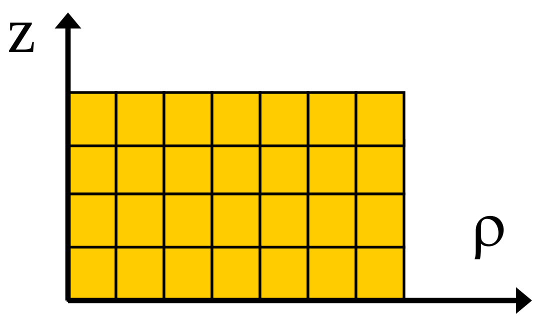

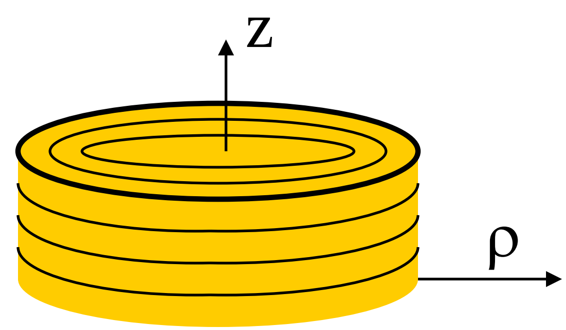

10nm transition layer from ρ=40 to 50nm.
Linear variation of ε.
Tensor effective medium representation:

$$\boldsymbol{\varepsilon} = \varepsilon_{\parallel}\left(\mathbf{I} - \hat{n}\hat{n}\right) + \varepsilon_{\perp}\hat{n}\hat{n}$$

$$\varepsilon_{\parallel} = \frac{1}{A}\int_A \varepsilon(\rho, z)\,dS$$

$$\frac{1}{\varepsilon_{\perp}} = \frac{1}{A}\int_A \frac{1}{\varepsilon(\rho, z)}\,dS$$

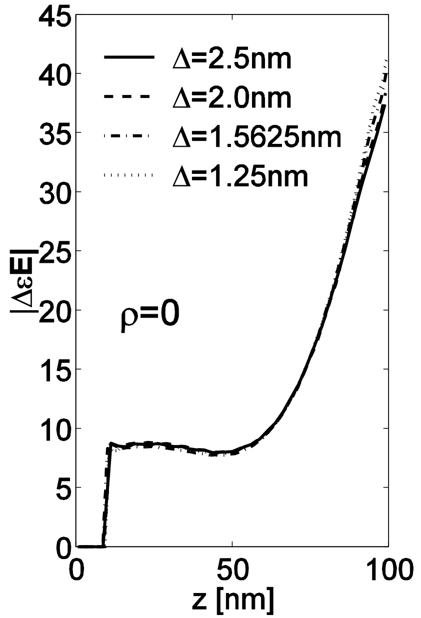

10nm transition layer from ρ=40 to 50nm.
Linear variation of ε.
Geometric averaging

$$\varepsilon = \frac{1}{A}\int_A \varepsilon(\rho, z)\,dS$$

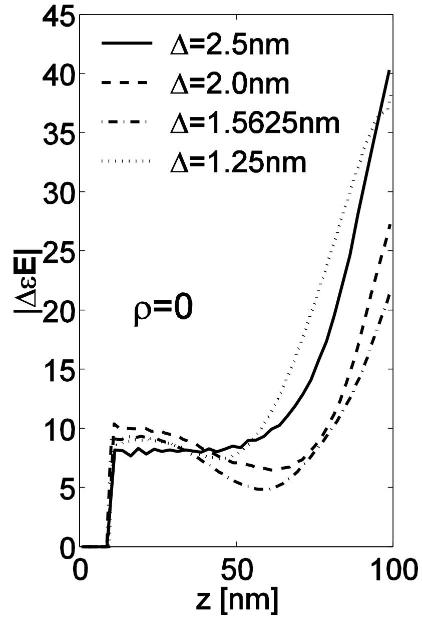

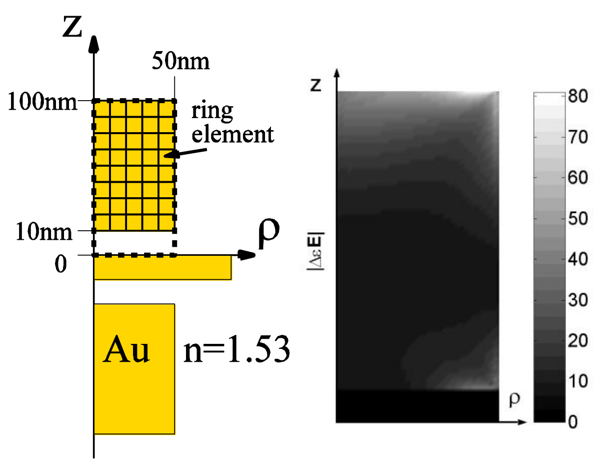

Sharp edge - no averaging:

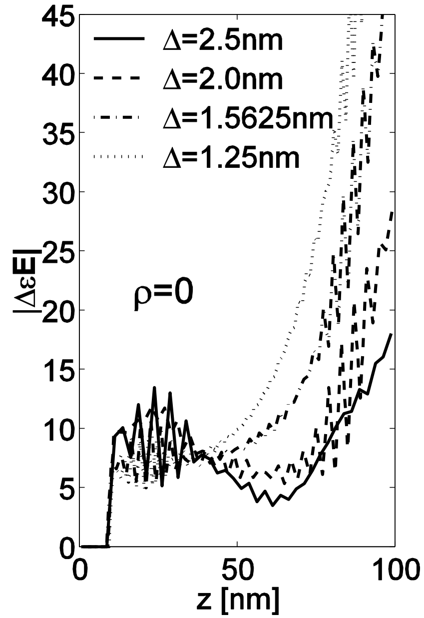

Green's tensor volume integral equation method (VIEM): Finite-size surface plasmon polariton bandgap structures

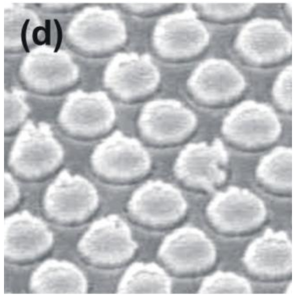

Modeling of a single scatterer required 5000-30000 discretization elements for each angular momentum. If we then also have several thousand scatterers an approximation method is required.

1) The incident field is assumed constant over a surface scatterer

2) The field inside a single scatterer ($\mathbf{A}_x$, $\mathbf{A}_y$ and $\mathbf{A}_z$) is calculated for an incident field being constant over the scatterer and oriented along each of the three main directions

3) The results for a single scatterer is reused in an approximation method for an array of a large number of scatterers ($E_{i,ext}$ is the external field at the site of a scatterer):

$$\mathbf{E}_{i,ext} \approx \mathbf{E}_{0,i} + \sum_{j \neq i} \int_{V_j} \mathbf{G}(\mathbf{r}_i, \mathbf{r}') k_0^2 \cdot \mathbf{P}_j(\mathbf{r}') d^3 r'$$

$$\mathbf{P}_i(\mathbf{r}) \approx \left(\mathbf{A}_x(\mathbf{r} - \mathbf{r}_i)\hat{x} + \mathbf{A}_y(\mathbf{r} - \mathbf{r}_i)\hat{y} + \mathbf{A}_z(\mathbf{r} - \mathbf{r}_i)\hat{z} \right) \cdot \mathbf{E}_{i,ext}$$

VIEM: Finite-size surface plasmon polariton bandgap structures

Gold particles arranged on a hexagonal lattice on a planar gold surface

The incident (but not the total) field is assumed constant across each scatterer

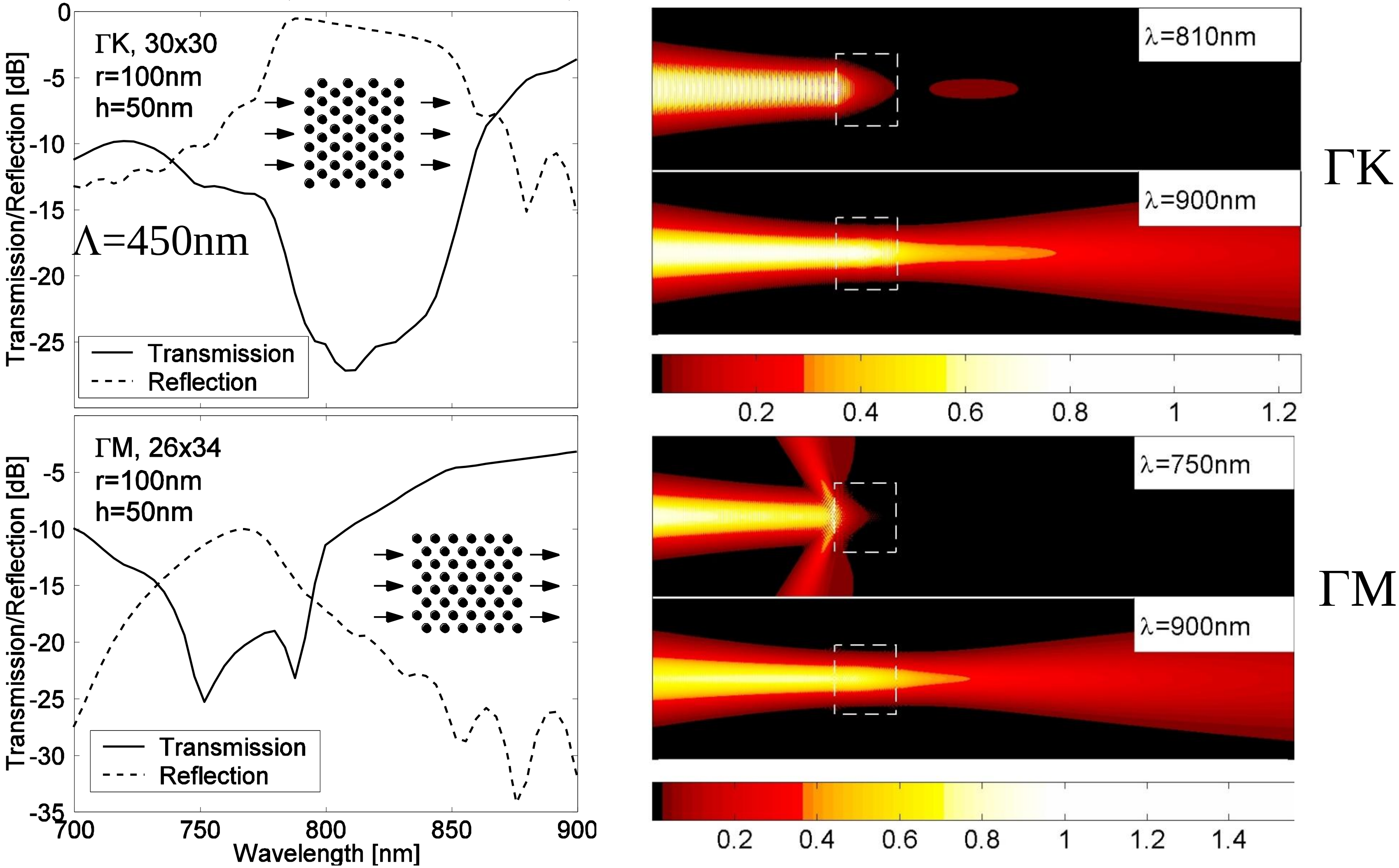

Bandgap vs size of surface scatterers

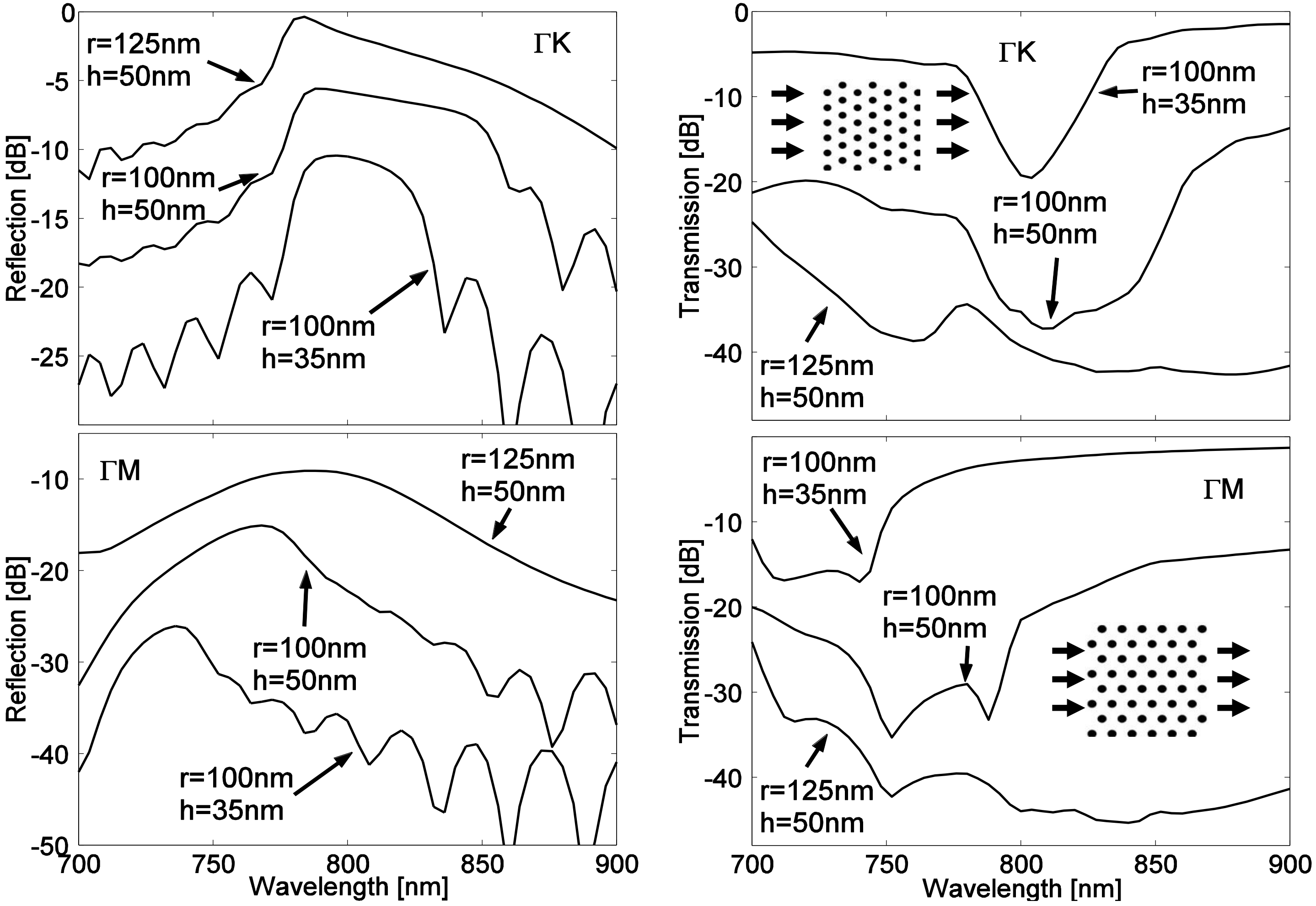

In-plane scattering

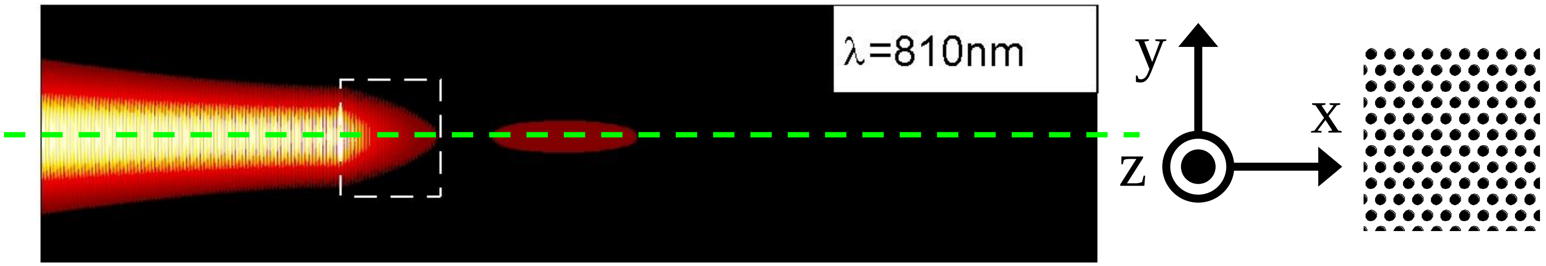

Out-of-plane scattering

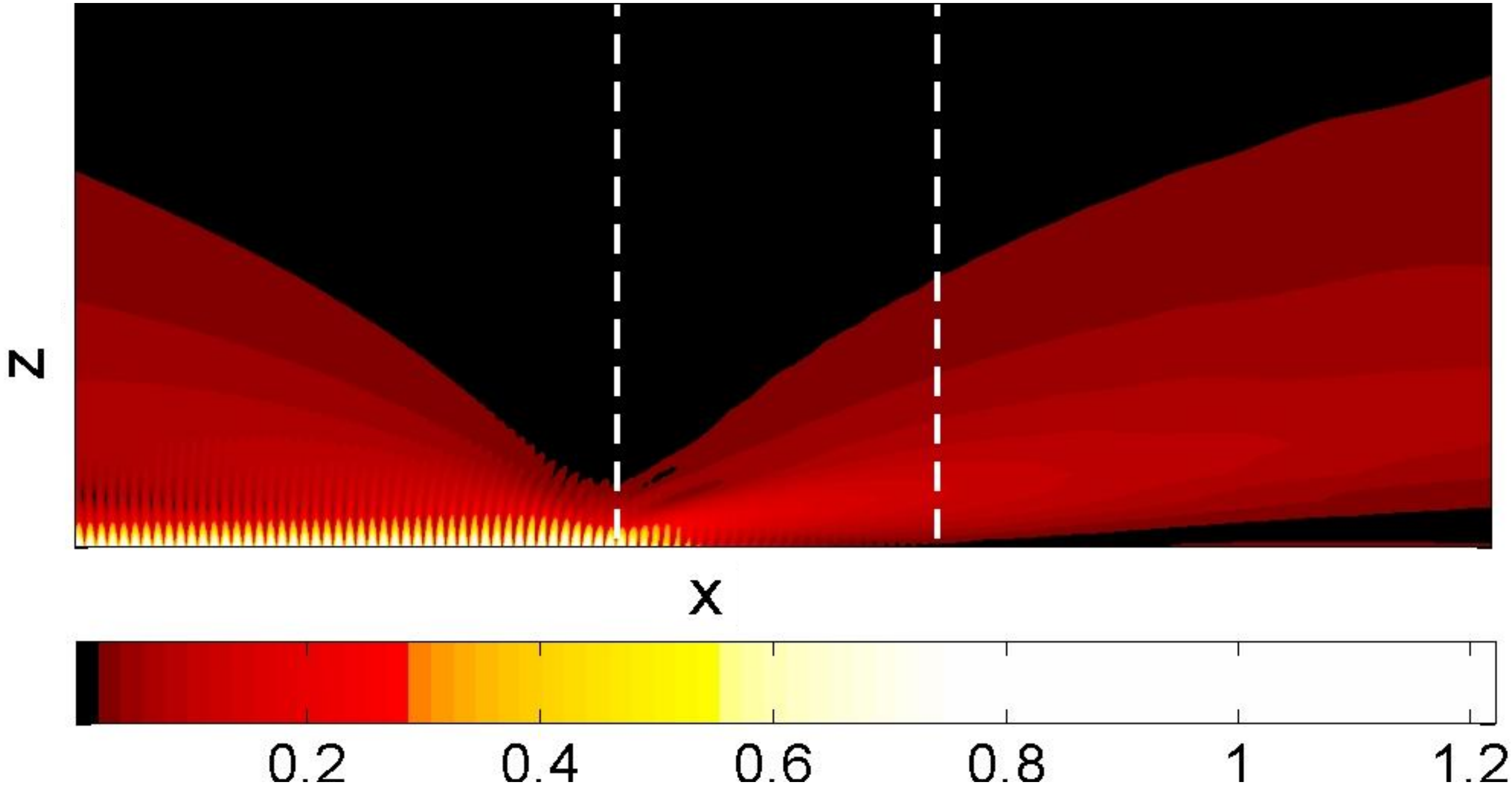

Transmission through a straight channel in a SPPBG structure

Particle size: h=50nm, r=125nm

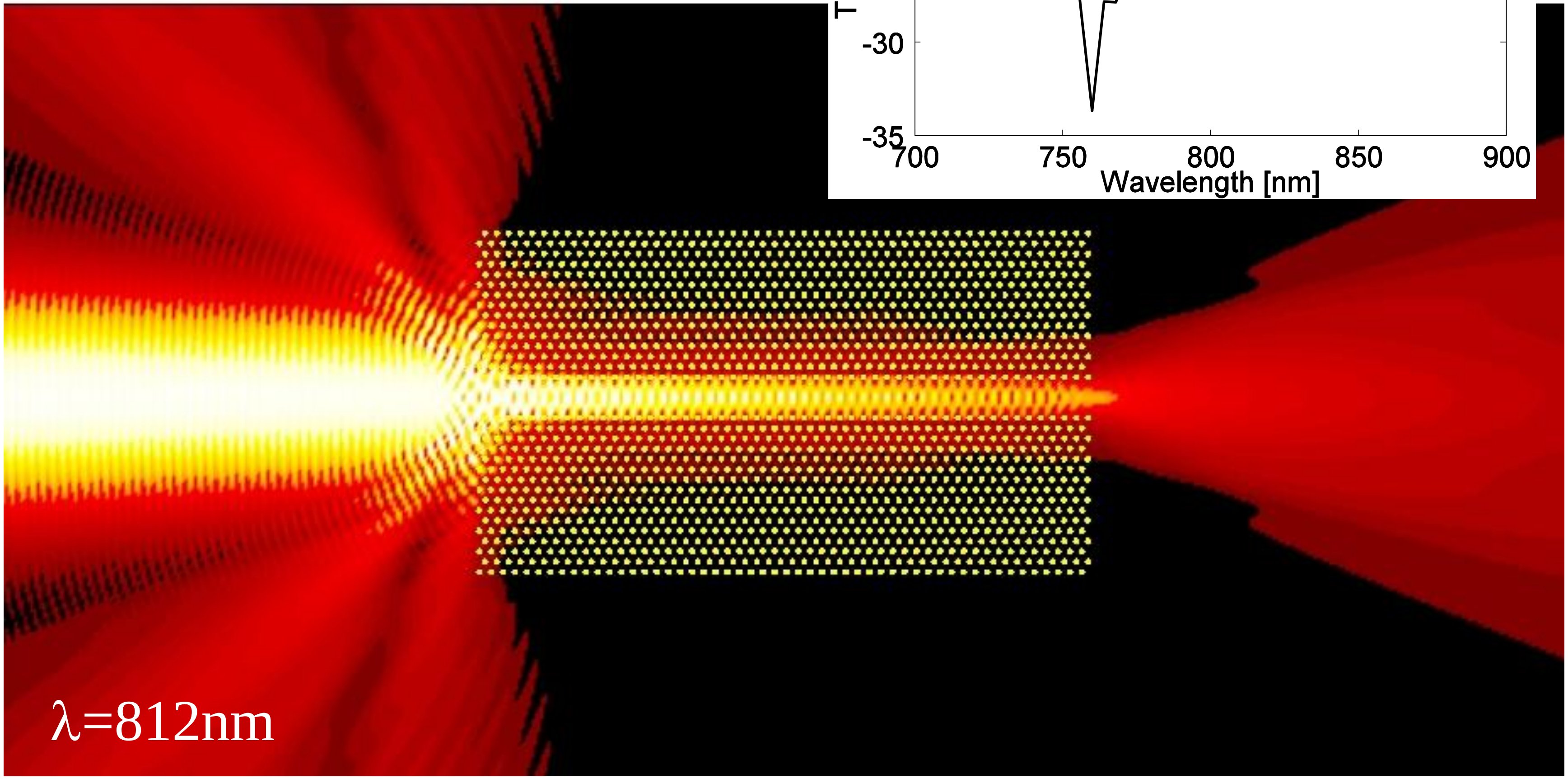

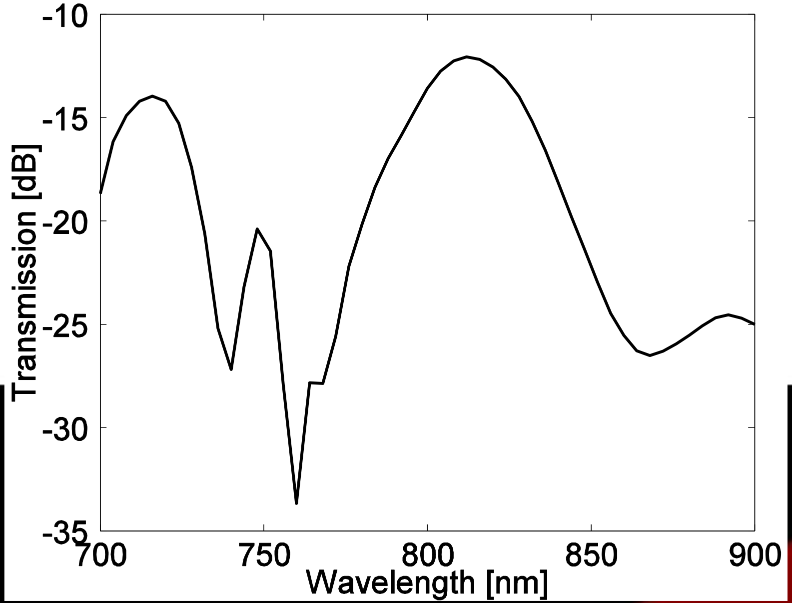

Transmission through a bent channel in a SPPBG structure

Particle size: h=50nm, r=125nm

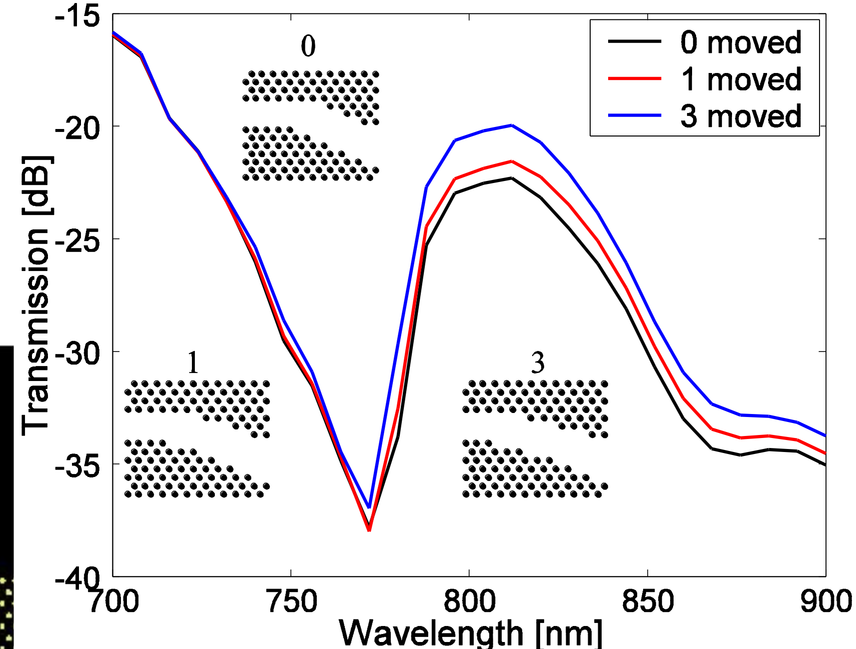

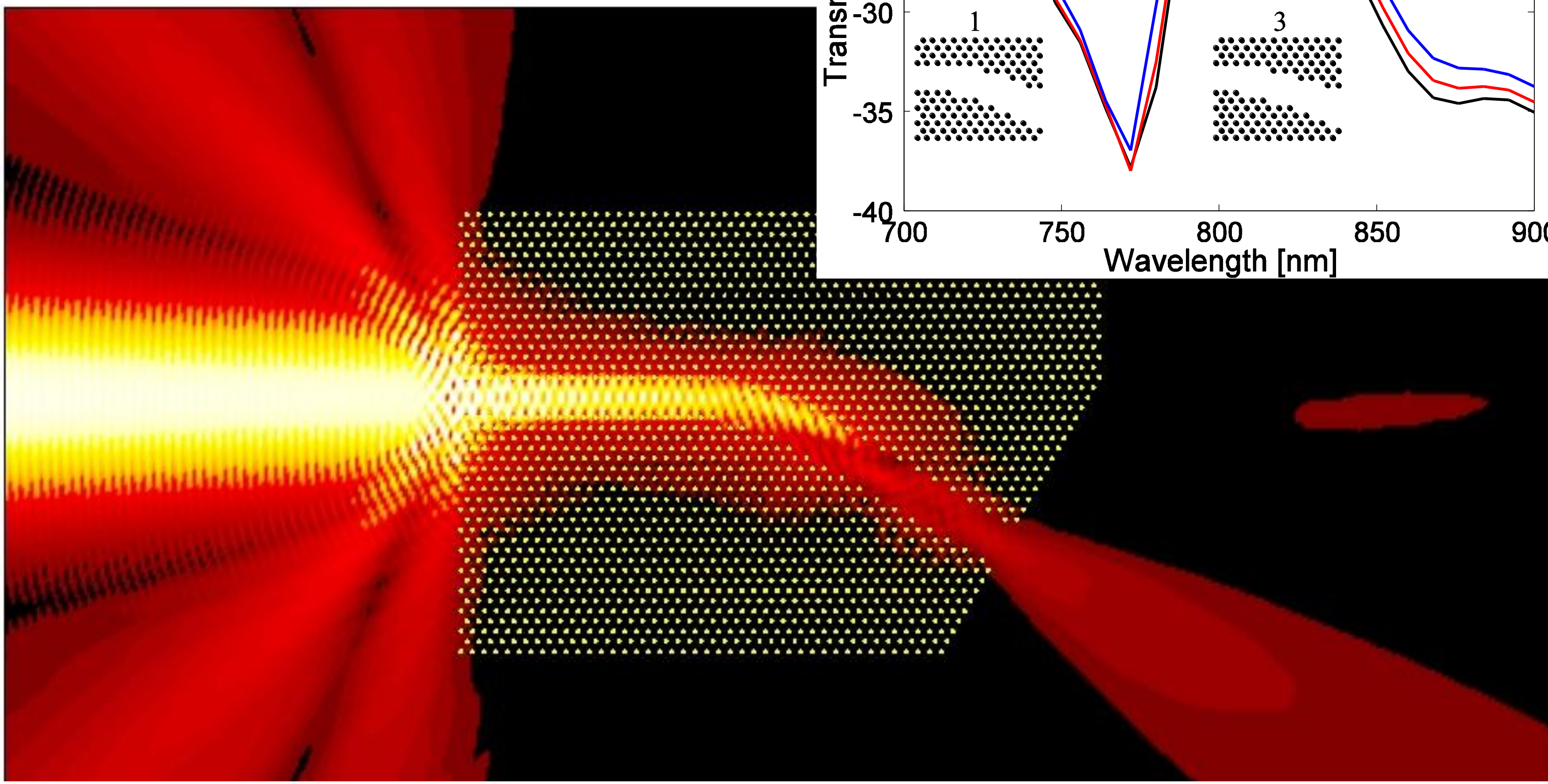

Transmission through a gradually bent channel (R=bend radius) in a SPPBG structure

Particle size: h=50nm, r=125nm

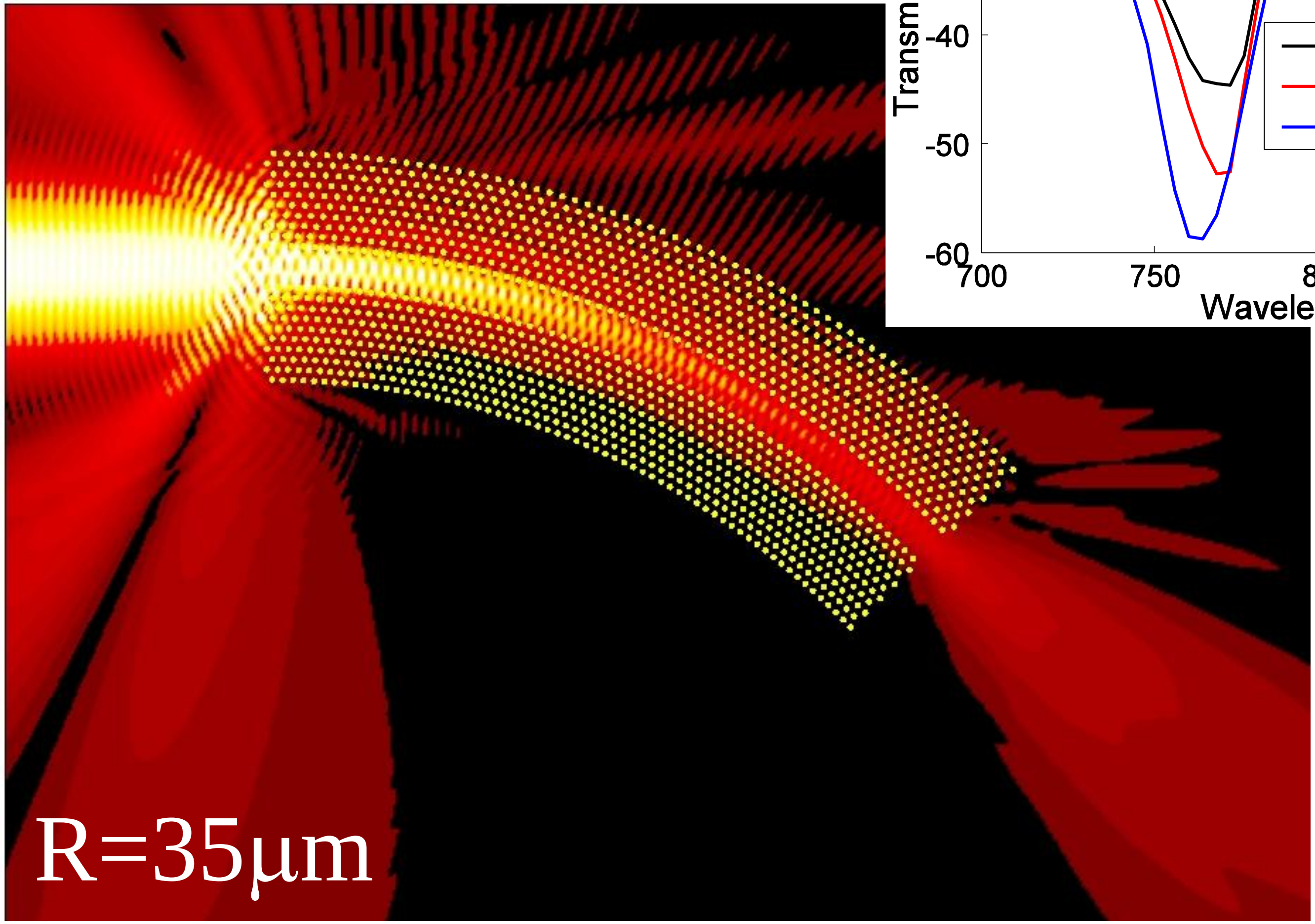

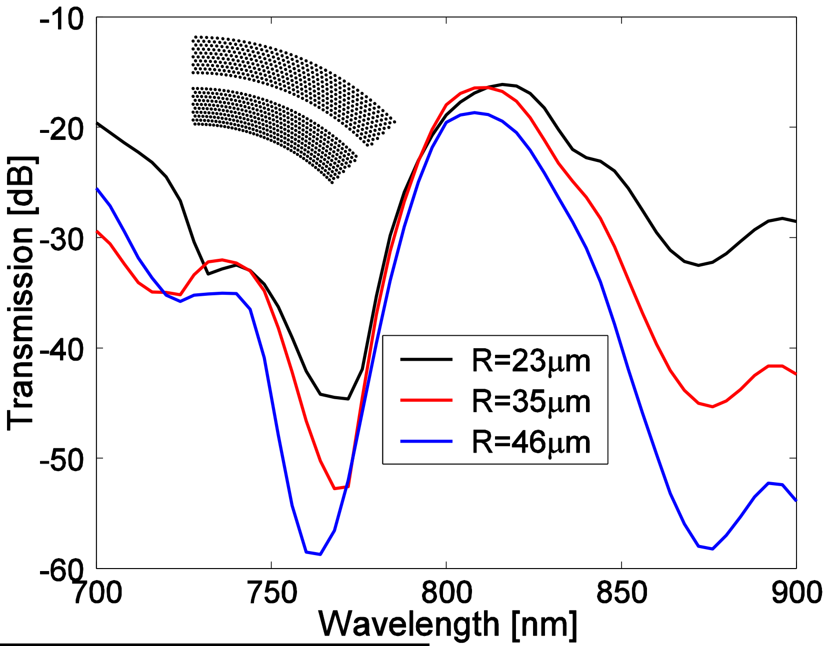

Green’s tensor area integral equation method (AIEM):

Homogeneous reference medium, p-polarization.

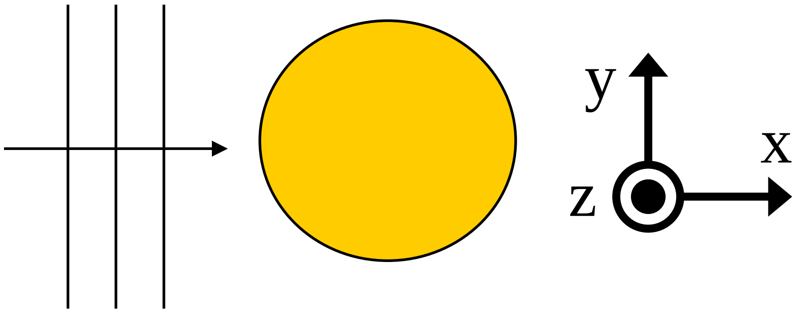

$$\mathbf{r} = \hat{x}x + \hat{y}y$$

$$\mathbf{E}(\mathbf{r}) = \hat{x}E_x(\mathbf{r}) + \hat{y}E_y(\mathbf{r})$$

The fields and the structure are assumed invariant along *z* (2D)

$$\mathbf{E}(\mathbf{r}) = \mathbf{E}_0(\mathbf{r}) + \int \mathbf{G}^D(\mathbf{r},\mathbf{r}')\mathrm{k}_0^2\left(\varepsilon(\mathbf{r}') - \varepsilon_{\mathrm{ref}}\right)\cdot \mathbf{E}(\mathbf{r}')\mathrm{d}^2\mathrm{r}'$$

$$\mathbf{G}^D(\mathbf{r},\mathbf{r}') = \left(\frac{1}{k^2}\nabla\nabla + \mathbf{I}\right) g^D(\mathbf{r},\mathbf{r}') \quad , \quad g^D(\mathbf{r},\mathbf{r}') = \frac{-i}{4}H_0^{(2)}\left(k|\mathbf{r}-\mathbf{r}'|\right)$$

Green's tensor area integral equation method (AIEM): Stair-cased description of surface vs using special surface elements

For a modest ratio of dielectric constants (=4) both methods converge.
Using special discretization elements near the surface that follow closely the surface profile offers a very significant improvement

Static limit: $\mathbf{E} = \mathbf{E}_0 2/(1+\varepsilon) = 0.4\mathbf{E}_0$

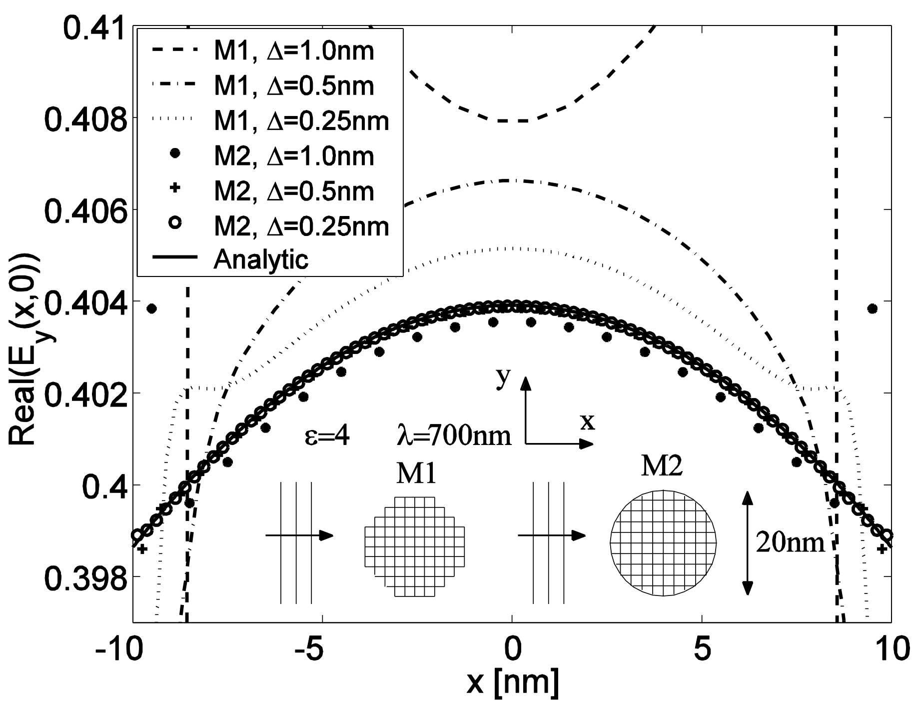

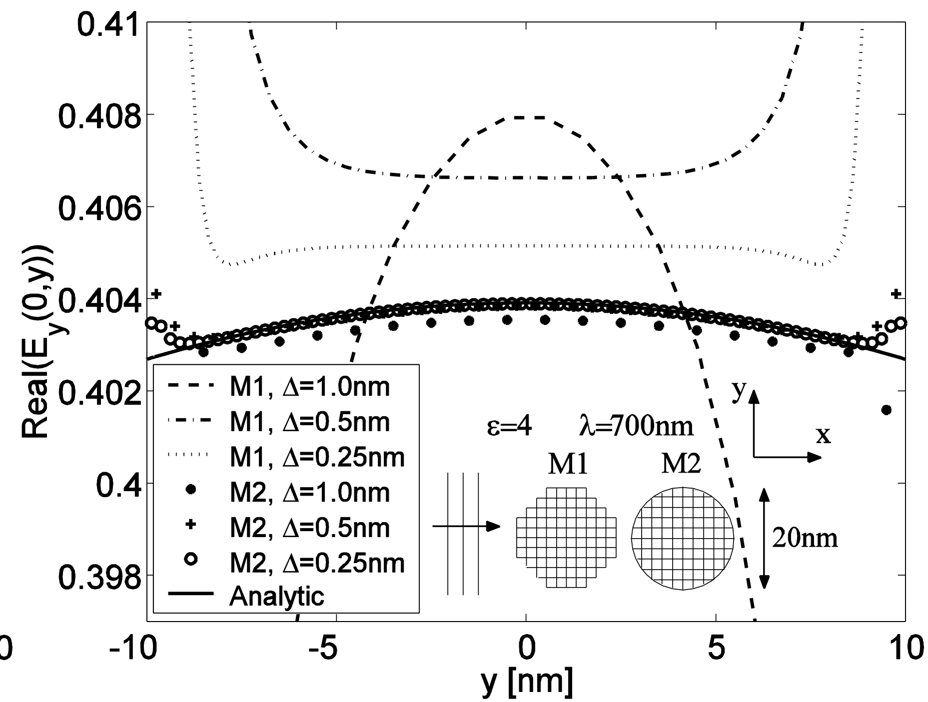

Green's tensor area integral equation method (AIEM): Stair-cased description of surface vs using special surface elements

For a large ratio of dielectric constants (1 : -22.99-i*0.395) the method of using a stair-cased description of the surface converges very slowly – if at all.

Reasonably efficient convergence is, however, achieved when using the special surface elements. In this case the numerical equations do not involve a discrete convolution and we cannot take advantage of the FFT to the same extent.

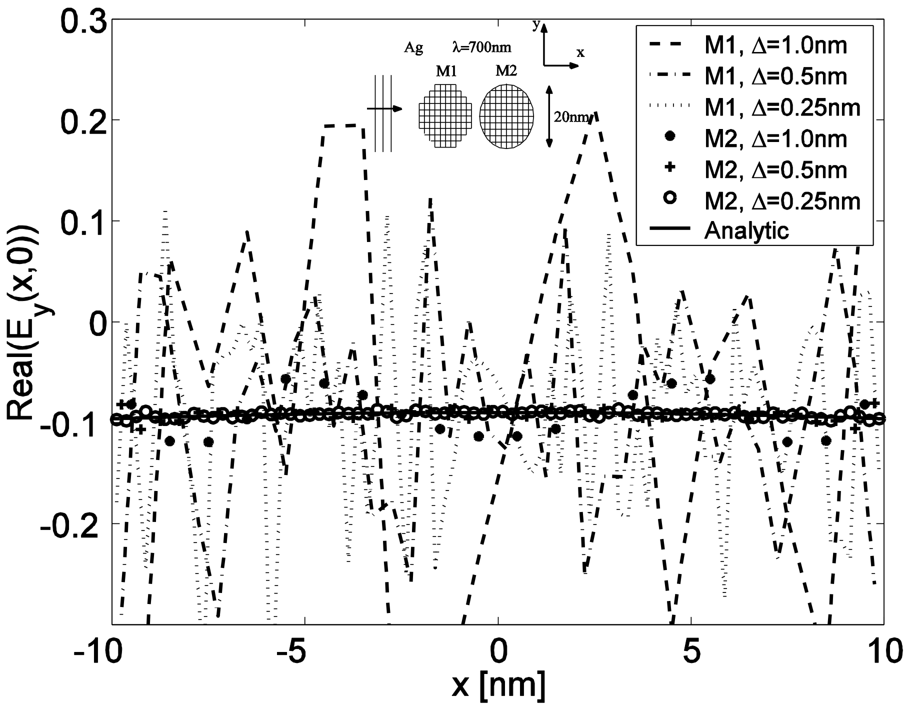

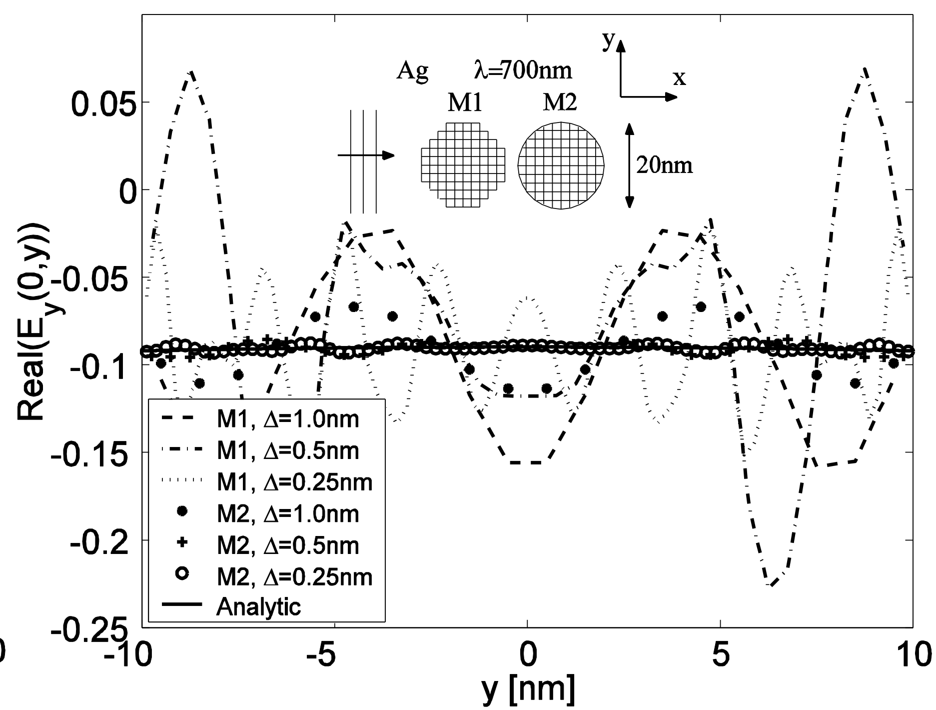

Ridge gratings for long-range surface plasmon polaritons

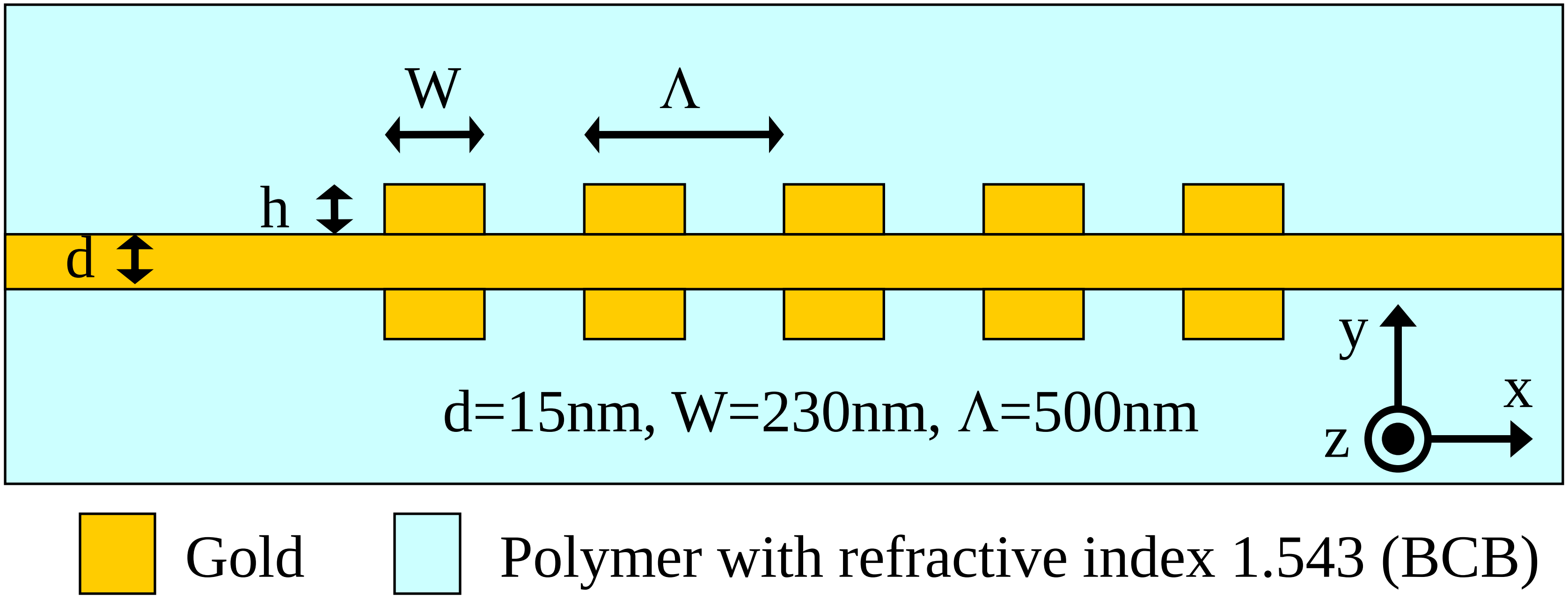

$$\mathbf{E}(\mathbf{r}) = \mathbf{E}_0(\mathbf{r}) + \int \mathbf{G}(\mathbf{r},\mathbf{r}')k_0^2\left(\varepsilon(\mathbf{r}') - \varepsilon_{ref}\right)\cdot \mathbf{E}(\mathbf{r}')d^2r'$$

Here **G** is the Green's tensor for a thin metal-film reference structure

Surface plasmon polariton contribution to Green's tensor

$$\mathbf{G}^{2D}_{LR-SPP}(\mathbf{r},\mathbf{r}') \approx A e^{-ik_{LR-SPP}|x-x'|} e^{-i\kappa_y (y+y')} \left(\hat{y}\hat{y} - \frac{\kappa_y^2}{\kappa_{LR-SPP}^2}\hat{x}\hat{x} + \frac{(x-x')}{|x-x'|}\frac{\kappa_y}{\kappa_{LR-SPP}}\left(\hat{y}\hat{x} - \hat{x}\hat{y}\right) \right)$$

$$y, y' > 0 \quad , \quad k_{LR-SPP}|x-x'| >> 1, \quad |x-x'| >> y+y'$$

We have found a long analytical expression for *A* – and similar expressions for the three-dimensional case using an eigenmode expansion of the Green's tensor:

$$\mathbf{G}^{2D}_{LR-SPP} = \sum_{LR\text{-}SPP \ \ states} \frac{|\phi_n\rangle\langle\phi_n|}{\lambda_n}$$

Evaluation of transmitted LR-SPP field (x-x'>0):

$$\mathbf{E}_{LR\text{-}SPP}(\mathrm{x},\mathrm{y}) \approx \mathbf{E}_{0,LR\text{-}SPP}(\mathbf{r}) + \int \mathbf{G}^{2D}_{LR-SPP}(\mathbf{r},\mathbf{r}')\mathrm{k}_0^2\left(\varepsilon(\mathbf{r}') - \varepsilon_{\mathrm{ref}}(\mathbf{r}')\right)\cdot\mathbf{E}(\mathbf{r}')\mathrm{d}^2\mathrm{r}'$$

Evaluation of reflected LR-SPP power (x-x'<0):

$$\mathbf{E}_{LR\text{-}SPP}(\mathrm{x},\mathrm{y}) \approx \int \mathbf{G}^{2D}_{LR-SPP}(\mathbf{r},\mathbf{r}')\mathrm{k}_0^2\left(\varepsilon(\mathbf{r}') - \varepsilon_{\mathrm{ref}}(\mathbf{r}')\right)\cdot\mathbf{E}(\mathbf{r}')\mathrm{d}^2\mathrm{r}'$$

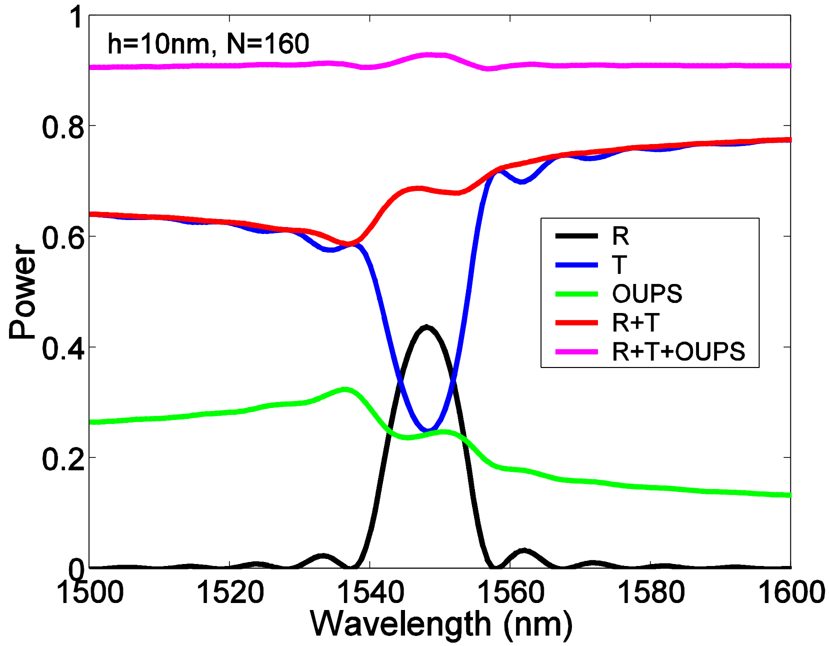

Double length

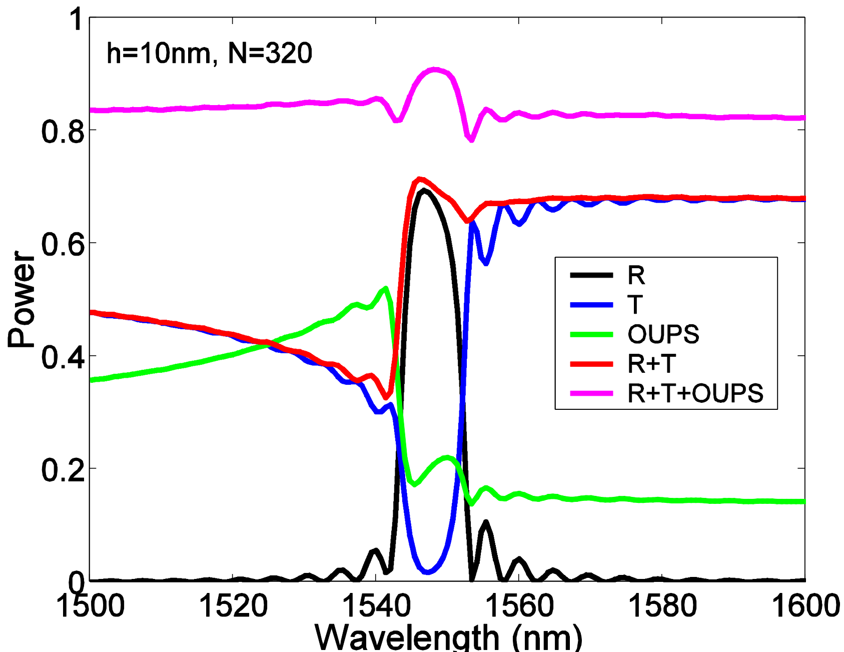

Double ridge height

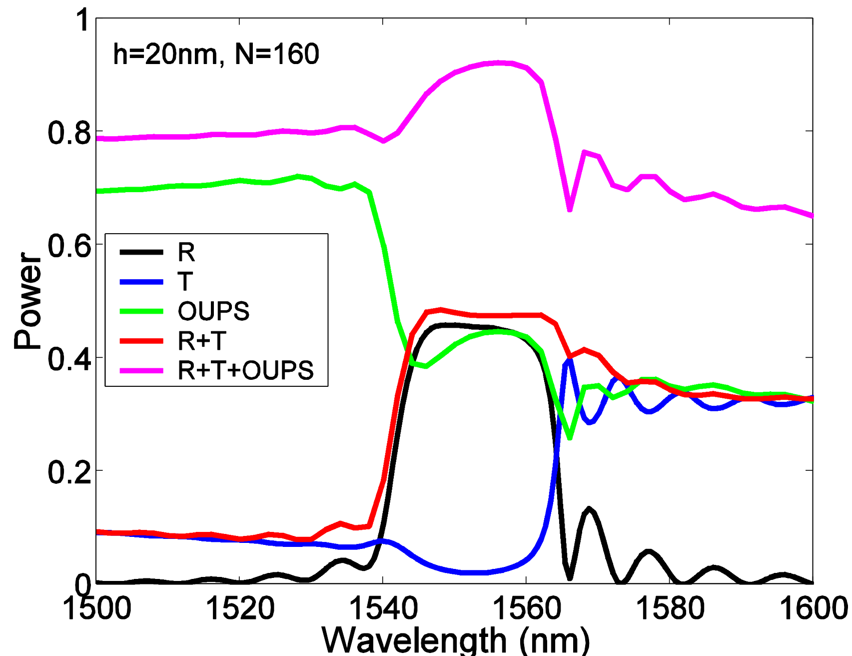

Light-line argument for large out-of-plane scattering for wavelengths below the bandgap

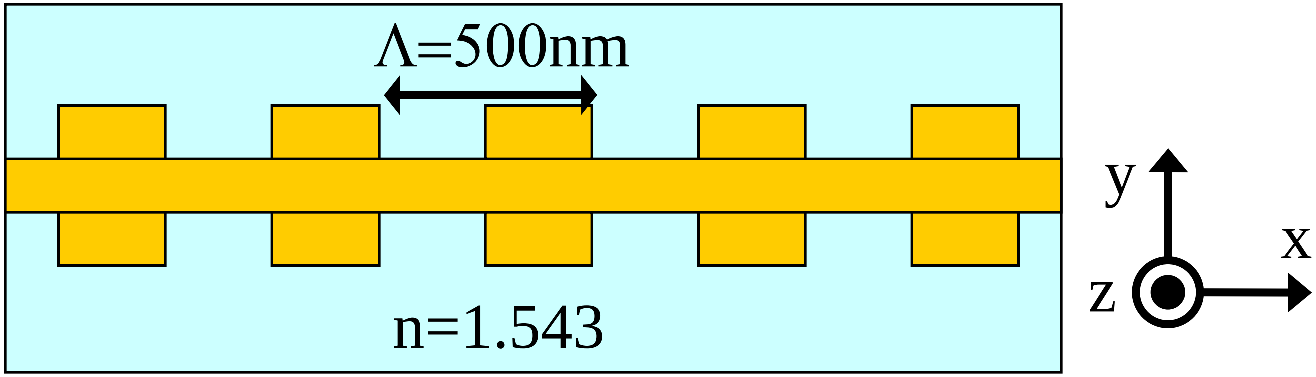

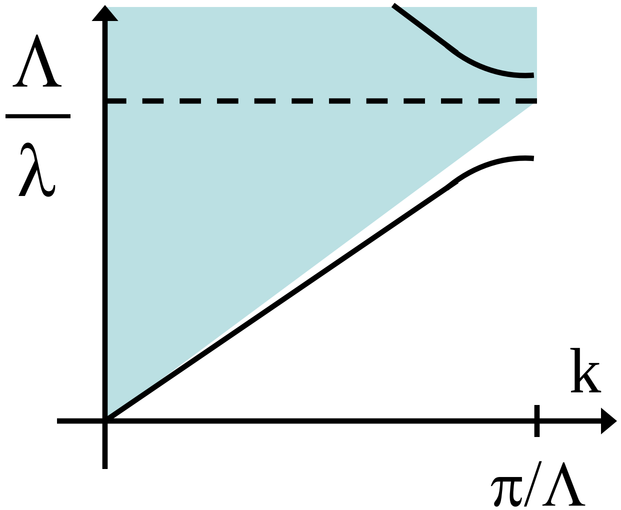

Bloch modes

$$\mathbf{E}_k(\mathbf{r}) = \mathbf{U}_k(\mathbf{r})e^{ikx}$$

Continuum of modes allowed to propagate in the polymer

Leakage-free guided modes do not exist for $\lambda < 2\Lambda n = 1543$nm

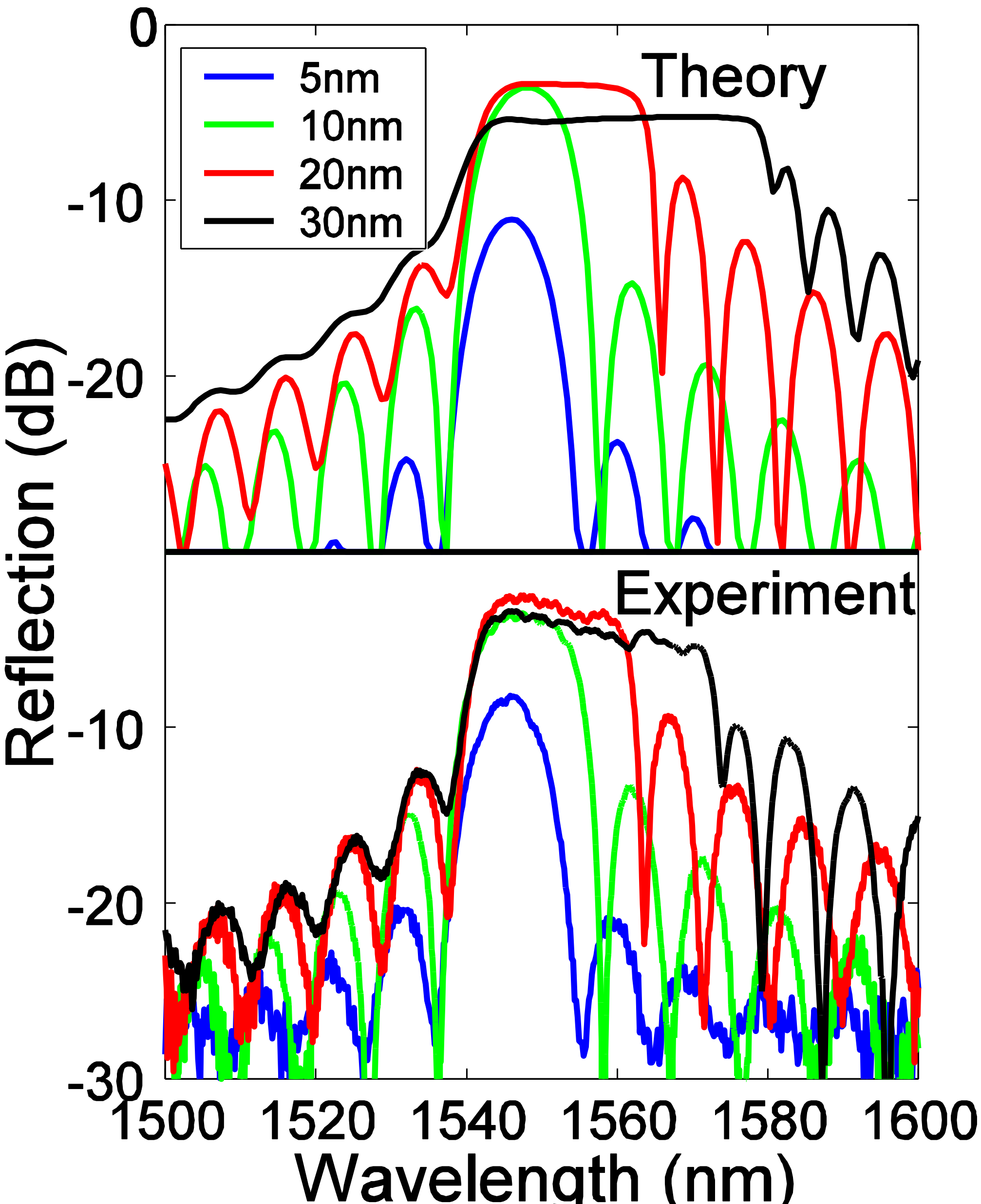

Case of 160 ridges:

Increasing the ridge height above a threshold leads to reduced peak reflection

The experiment was made by A. Boltasseva

Ref.: T. Søndergaard, S.I. Bozhevolnyi, and A. Boltasseva, Phys. Rev. B **73**, 045320 (2006).

Case of ridge height h=10nm.
Theory versus experiments for different grating lengths

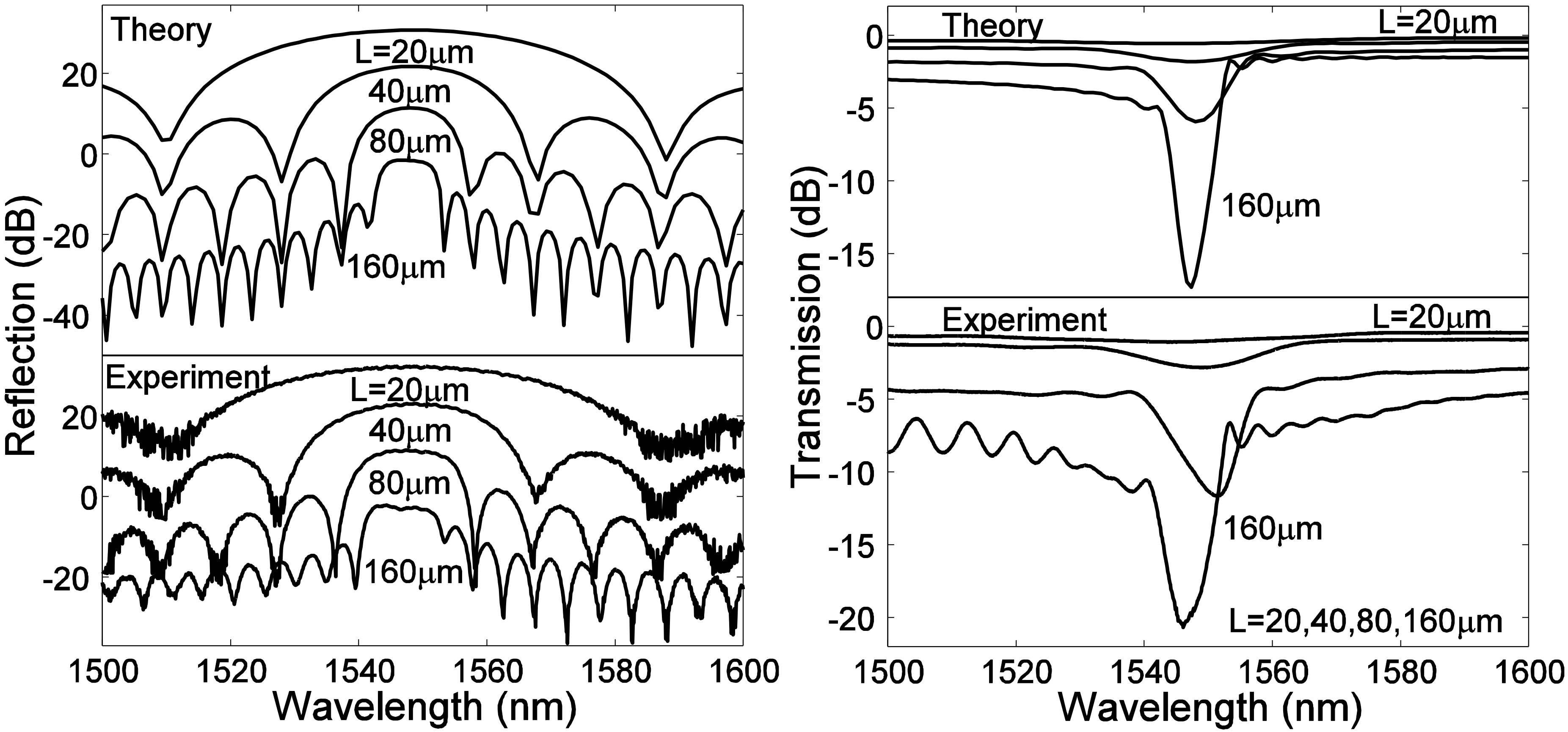

Ref.: S.I. Bozhevolnyi, A. Boltasseva, T. Søndergaard, T. Nikolajsen, and K. Leosson, Optics Communications **250**, 328-33 (2005).

Green's function surface integral equation method

$$\mathbf{H}(\mathbf{r}) = \hat{z}H(\mathbf{r}) = \hat{z}H_0(\mathbf{r}) + \hat{z}H_{scat}(\mathbf{r}) \ ,$$

$$\mathbf{r} = x\hat{x} + y\hat{y}$$

$$g_{1,2}(\mathbf{r},\mathbf{r}') = \frac{1}{4i} H_0^{(2)}\left(k_0 \sqrt{\varepsilon_{1,2}}\,|\mathbf{r}-\mathbf{r}'|\right)$$

$$\left(\nabla^2 + k_0^2 \varepsilon_{1,2}\right) g_{1,2}(\mathbf{r},\mathbf{r}') = -\delta(\mathbf{r}-\mathbf{r}')$$

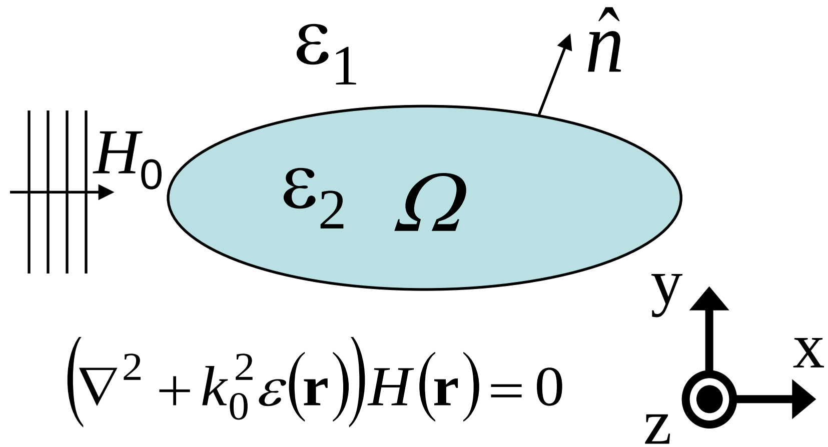

$$\left(\nabla^2 + k_0^2 \varepsilon(\mathbf{r})\right) H(\mathbf{r}) = 0$$

The magnetic field at any position can be obtained from surface integrals

$$H(\mathbf{r}) = H_0(\mathbf{r}) + \oint_{\partial\Omega} \left\{ H(\mathbf{s}')\hat{n}'\cdot\nabla' g_1(\mathbf{r},\mathbf{s}') - g_1(\mathbf{r},\mathbf{s}')\hat{n}'\cdot\nabla' H_1(\mathbf{s}') \right\} dl' \ , \ \mathbf{r} \notin \Omega$$

$$H(\mathbf{r}) = -\oint_{\partial\Omega} \left\{ H(\mathbf{s}')\hat{n}'\cdot\nabla' g_2(\mathbf{r},\mathbf{s}') - g_2(\mathbf{r},\mathbf{s}')\frac{\varepsilon_2}{\varepsilon_1}\hat{n}'\cdot\nabla' H_1(\mathbf{s}') \right\} dl' \ , \ \mathbf{r} \in \Omega$$

Self-consistent equations:

$$\frac{1}{2}H(\mathbf{s}) = H_0(\mathbf{s}) + P\oint_{\partial\Omega} \left\{ H(\mathbf{s}')\hat{n}'\cdot\nabla' g_1(\mathbf{s},\mathbf{s}') - g_1(\mathbf{s},\mathbf{s}')\hat{n}'\cdot\nabla' H_1(\mathbf{s}') \right\} dl'$$

$$\frac{1}{2}H(\mathbf{s}) = -P\oint_{\partial\Omega} \left\{ H(\mathbf{s}')\hat{n}'\cdot\nabla' g_2(\mathbf{s},\mathbf{s}') - g_2(\mathbf{s},\mathbf{s}')\frac{\varepsilon_2}{\varepsilon_1}\hat{n}'\cdot\nabla' H_1(\mathbf{s}') \right\} dl'$$

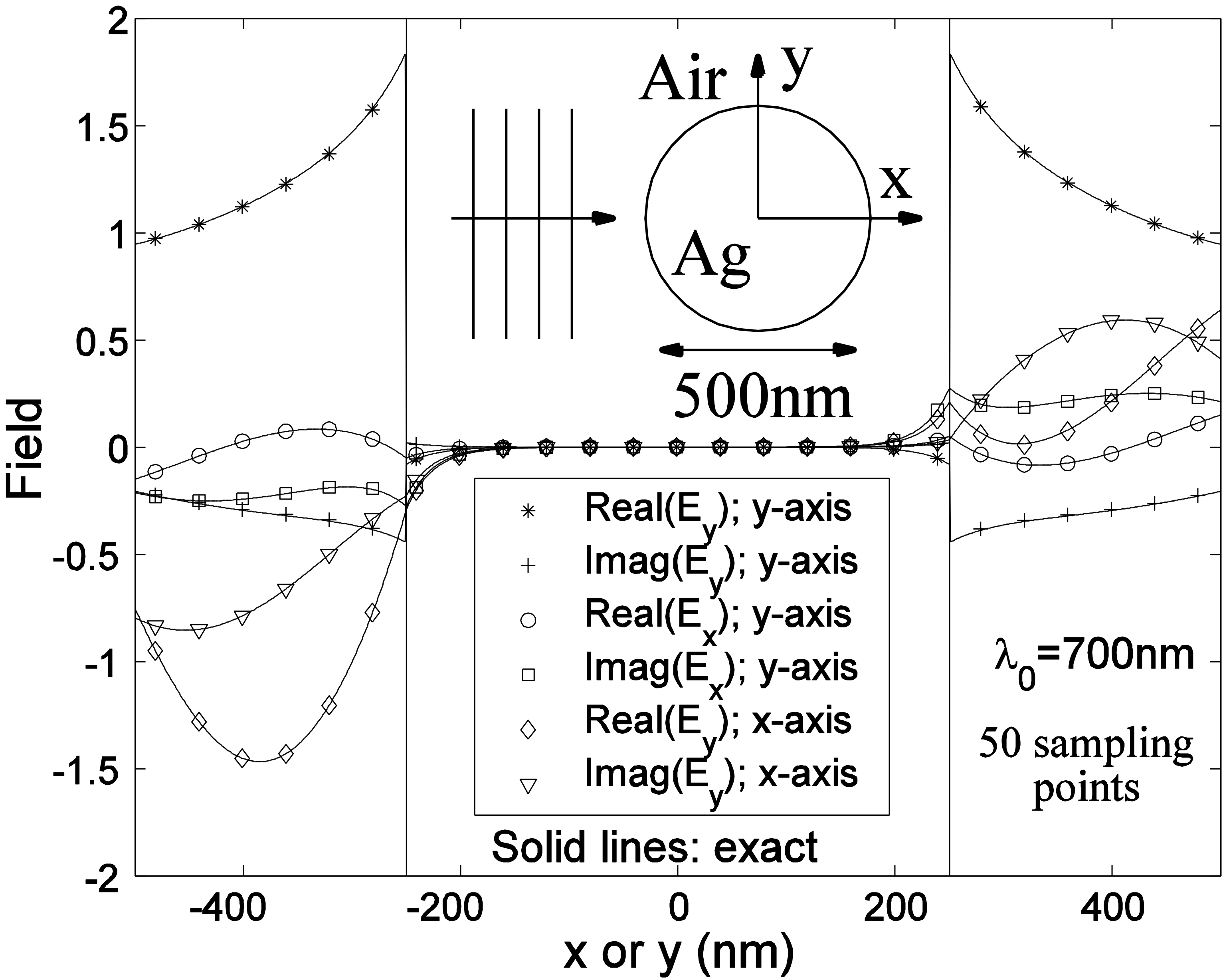
Air
y
x
Ag
500nm
Real(E_y); y-axis
Imag(E_y); y-axis
Real(E_x); y-axis
Imag(E_x); y-axis
Real(E_y); x-axis
Imag(E_y); x-axis
λ_0=700nm
50 sampling points
Solid lines: exact
Field
x or y (nm)
2
1.5
1
0.5
0
-0.5
-1
-1.5
-2
-400
-200
0
200
400

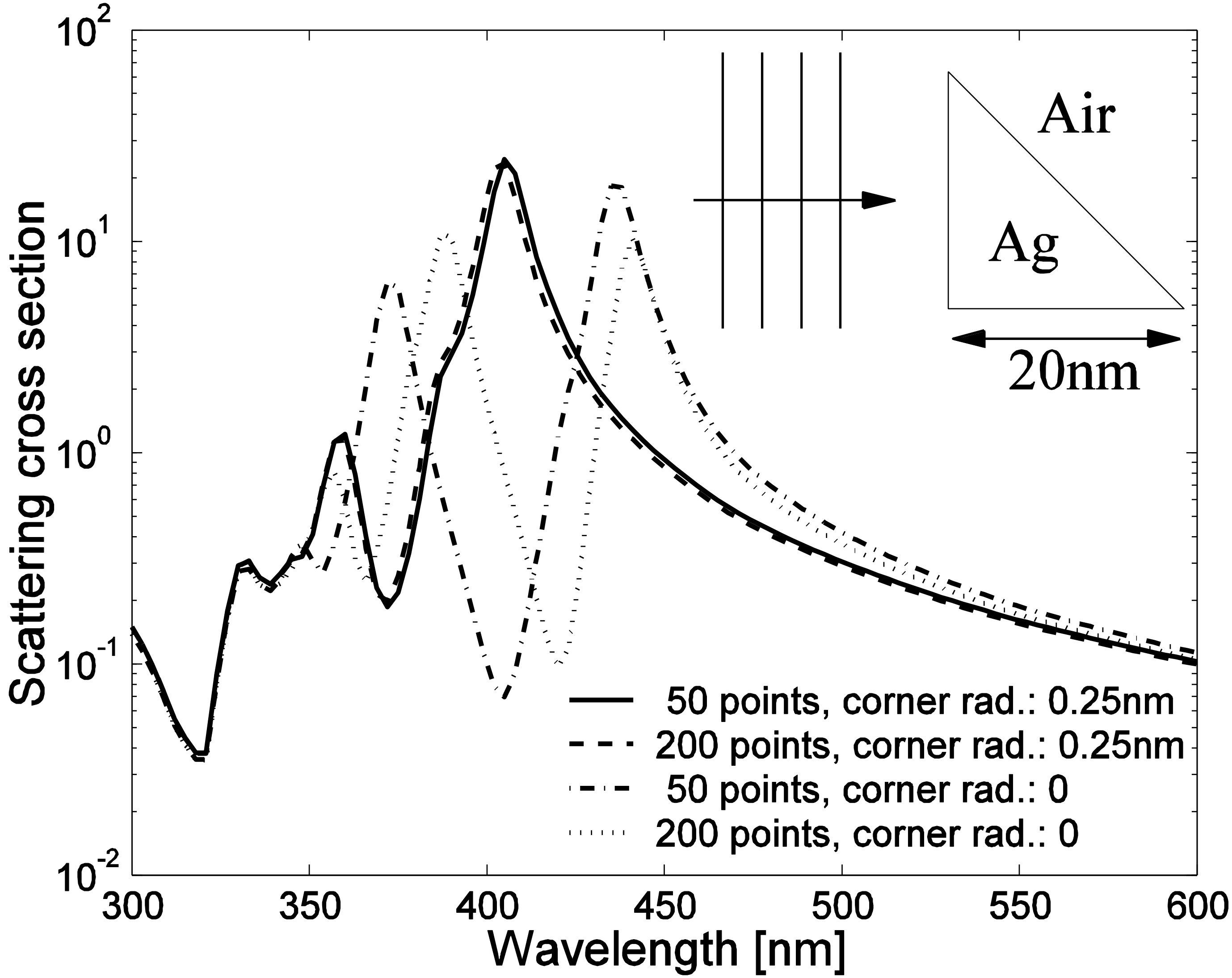

Quantitative agreement with: J.P. Kottmann et al., Opt. Express **6**, 213 (2000).

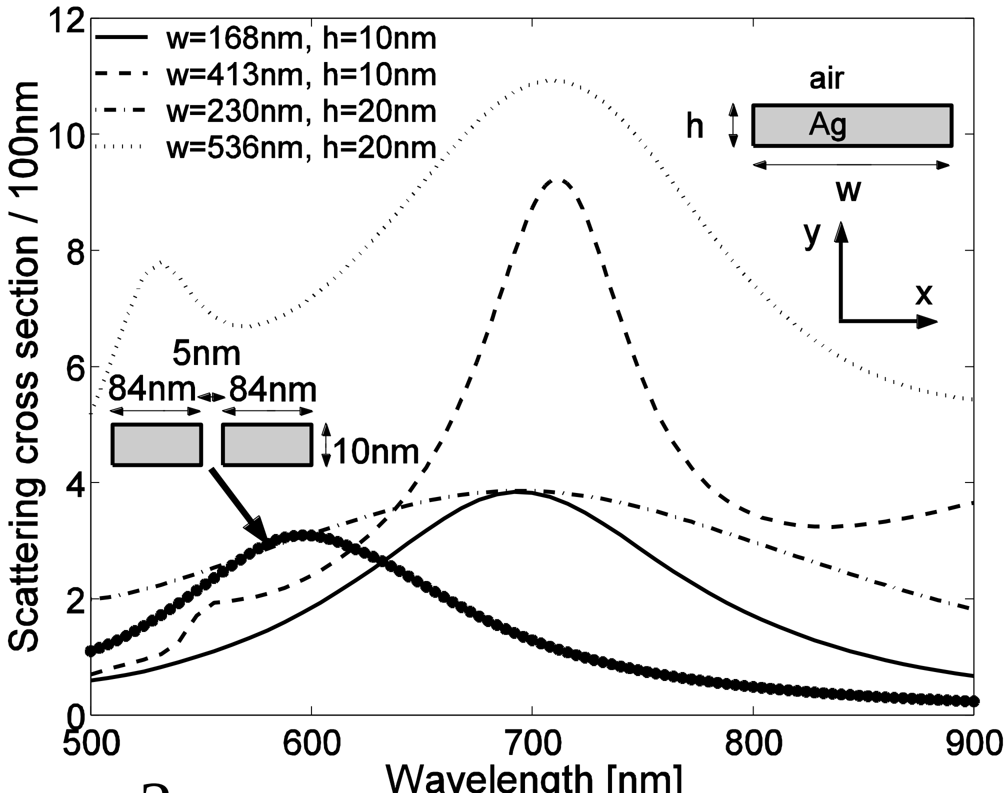

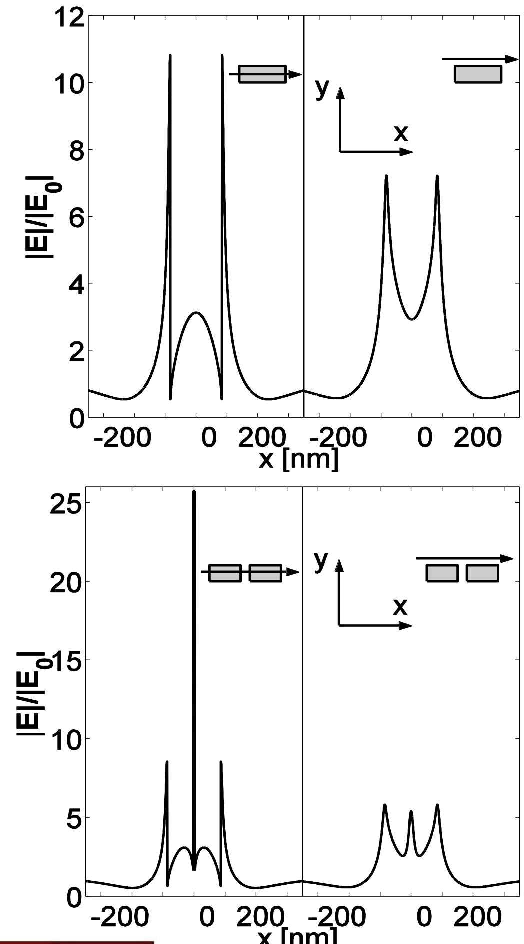

$$w\frac{2\pi}{\lambda}n_{slow} = m\pi - \phi$$

θ=45°

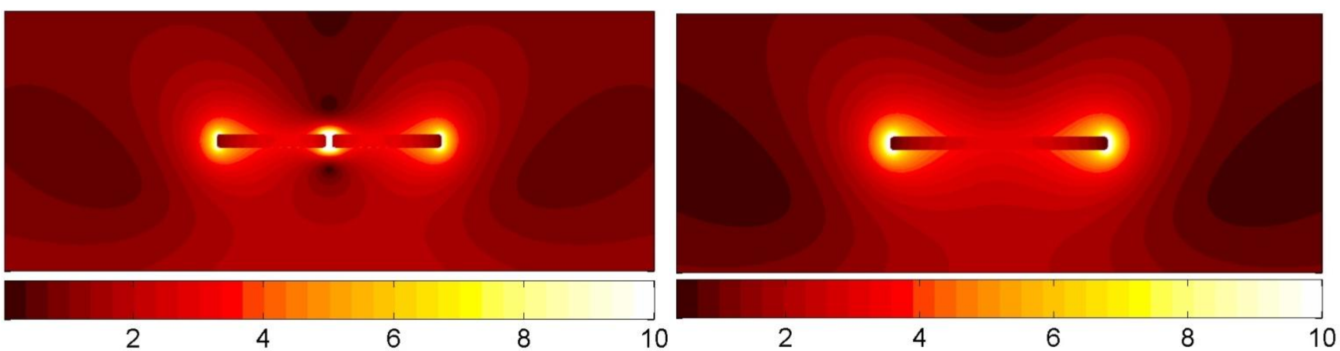

Electric field magnitude enhancement (values >10 are set to 10)

Ref.: T. Søndergaard, and S.I. Bozhevolnyi, Phys. Stat. Sol. (b) **245**, 9-19 (2008).

AALBORG UNIVERSITY

Summary

The treatment of the surface of plasmonic (metal) nano structures is crucial.

VIEM:

· Cubic volume elements for a cylindrical gold scatterer did not work at all.
· Ring volume elements and a cylindrical harmonic field expansion worked - but only when using ”soft” edges.
· The result for a single scatterer was reused in an approximation method for large arrays of scatterers (SPPBG structures).

AIEM:

· Square area elements did not work for a circular metal cylinder.
The method became efficient when replacing elements near the surface with special elements following closely the shape of the structure surface.
· The method was applied to LR-SPP ridge gratings.

SIEM:

· Rounding of sharp corners may be necessary.
· The method was exemplified for metal nano-strip resonators.

(The methods are reviewed in: T. Søndergaard, phys. stat. Sol. (b) **244**, 3448-62 (2007).

Exercises:

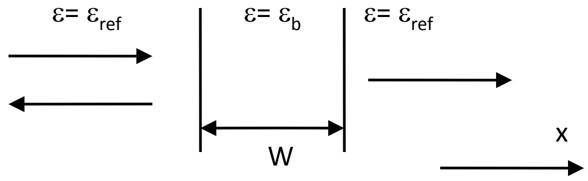

$$E(x) = E_0(x) + \int g(x, x')k_0^2\left(\varepsilon(x') - \varepsilon_{ref}\right)E(x')dx'$$

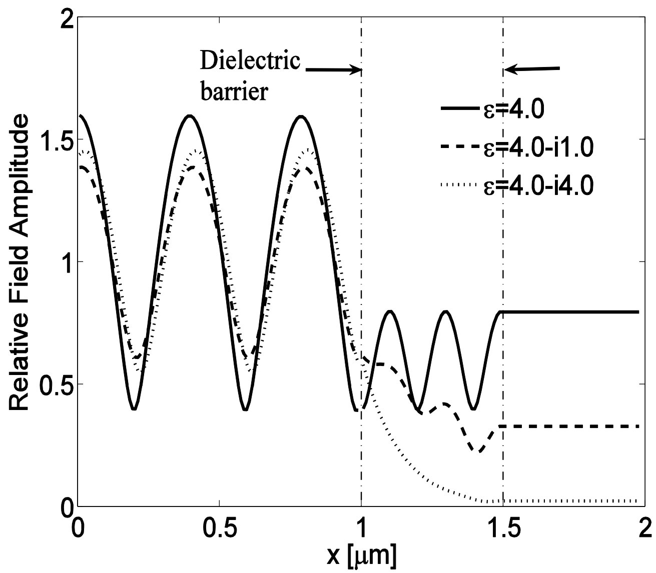

Thomas Søndergaard, October 27, 2008

Exercises:

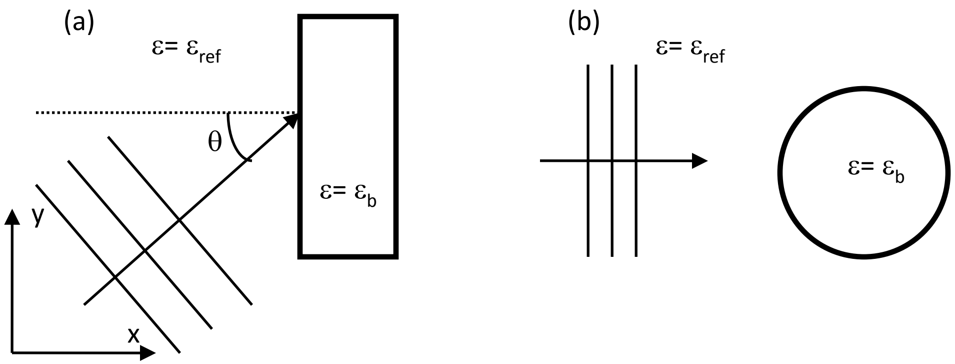

$$E(x,y) = E_0(x,y) + \int g(x,y;x',y')k_0^2\left(\varepsilon(x',y') - \varepsilon_{ref}\right)E(x',y')dx'dy'$$

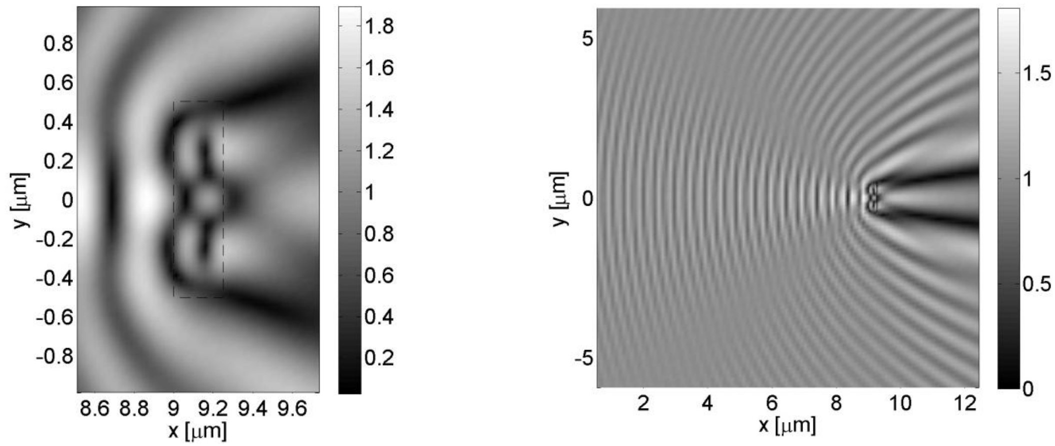

Thomas Søndergaard, October 27, 2008

Acknowledgements - people:

Sergey I. Bozhevolnyi
Jonas Beermann
Alexandra Boltasseva
Thomas Nikolajsen
Kristjan Leosson
Jesper Jung

Acknowledgements - projects:

The Danish Research Council for Technology and Production

The NABIIT project financed by the Danish Research Agency (contract 2106-05-033)